

ตัวเร่งปฏิกิริยาวิวิธพันธุ์สำหรับการผลิตไบโอดีเซลจากน้ำมันพืชที่มีกรดไขมันอิสระสูง



นางสาวพัชรรณณ์ ช่วยปลอด

สถาบันวิทยบริการ

จุฬาลงกรณ์มหาวิทยาลัย

วิทยานิพนธ์นี้เป็นส่วนหนึ่งของการศึกษาตามหลักสูตรปริญญาวิทยาศาสตรมหาบัณฑิต

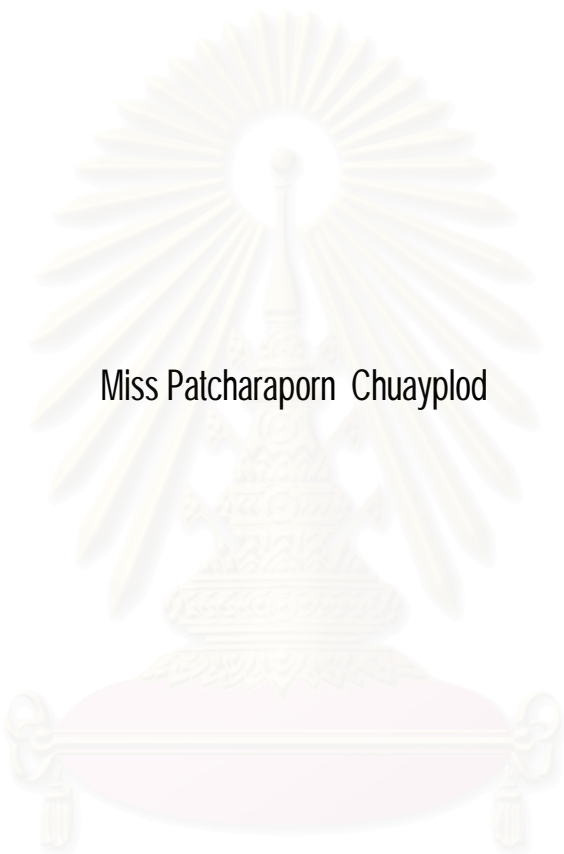
สาขาวิชาปิโตรเคมีและวิทยาศาสตร์พอลิเมอร์

คณะวิทยาศาสตร์ จุฬาลงกรณ์มหาวิทยาลัย

ปีการศึกษา 2550

ลิขสิทธิ์ของจุฬาลงกรณ์มหาวิทยาลัย

HETEROGENEOUS CATALYSTS FOR BIODIESEL PRODUCTION FROM HIGH FREE FATTY ACID
VEGETABLE OIL



Miss Patcharaporn Chuayplod

สถาบันวิทยบริการ
A Thesis Submitted in Partial Fulfillment of the Requirements
for the Degree of Master of Science Program in Petrochemistry and Polymer Science

Faculty of Science
Chulalongkorn University
Academic Year 2007

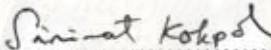
Copyright of Chulalongkorn University

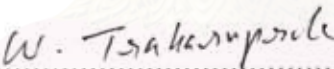
Thesis Title HETEROGENEOUS CATALYSTS FOR BIODIESEL PRODUCTION FROM
HIGH FREE FATTY ACID VEGETABLE OIL
By Miss. Patcharaporn Chuayplod
Field of study Petrochemistry and Polymer Science
Thesis Advisor Associate Professor Wimonrat Trakarnpruk, Ph.D.

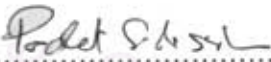
Accepted by the Faculty of Science, Chulalongkorn University in Partial
Fulfillment of the Requirements for the Master's Degree

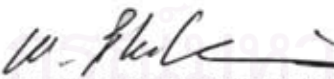

.....Dean of the Faculty of Science
(Professor Supot Hannongbua, Ph.D.)

THESIS COMMITTEE


.....Chairman
(Associate Professor Sirirat Kokpol, Ph.D.)


.....Thesis Advisor
(Associate Professor Wimonrat Trakarnpruk, Ph.D.)


..... External Member
(Professor Padet Sidsunthorn, Ph D.)


.....Member
(Assistant Professor Worawan Bhanthumnavin, Ph.D.)


.....Member
(Amarawan Intasiri, Ph.D.)

พัชรภรณ์ ช่วยปลอด: ตัวเร่งปฏิกิริยาวิวิธพันธุ์สำหรับการผลิตไบโอดีเซลจากน้ำมันพืชที่มีกรดไขมันอิสระสูง. (HETEROGENEOUS CATALYSTS FOR BIODIESEL PRODUCTION FROM HIGH FREE FATTY ACID VEGETABLE OIL)

อ.ที่ปรึกษา : รศ.ดร. วิมลรัตน์ ตระการพฤษ, 84 หน้า.

กระบวนการเร่งปฏิกิริยาแบบสองขั้นตอน ซึ่งประกอบด้วยปฏิกิริยาเอสเทอร์ฟิเคชันและทรานส์เอสเทอร์ฟิเคชันถูกนำมาใช้สำหรับการเปลี่ยนรูปของน้ำมันรำข้าวไปเป็นแผลตดีแอซิดเมทิลเอสเทอร์ (ไบโอดีเซล) โดยใช้ตัวเร่งปฏิกิริยากัดและเบส ขั้นแรก ทำการสังเคราะห์ตัวเร่งปฏิกิริยาเบสระบบวิวิธพันธุ์: MgAl ไฮโดรเทลไชต์ (สัดส่วนโดยโมล Mg/Al = 3 และ 4) MgAl ไฮโดรเทลไชต์ที่เผา (MgAlO) และใส่โลหะ (K, Cs, Sr, Ba, La) และ Mg(Al)La ไฮโดรเทลไชต์ และรีไฮเดรท Mg(Al)La ไฮโดรเทลไชต์ และตรวจสอบเอกลักษณ์ด้วย ICP, XRD, SEM, BET และ FT-IR วัดความเป็นเบสโดยการไทเทรชัน ใช้กลีเซอรอลโทรมิวทิเรตเป็นสารประกอบจำลองสำหรับทรานส์เอสเทอร์ฟิเคชันกับเมทานอล เพื่อเปรียบเทียบประสิทธิภาพในการเร่งปฏิกิริยาของตัวเร่งปฏิกิริยาผลการทดลองแสดงว่าในบรรดาออกไซด์ผสมที่ใส่โลหะ MgAlO ที่ใส่ 1.5 wt%K ให้ค่าการเปลี่ยนรูปสูงที่สุด อย่างไรก็ตามตรวจพบการหลุดออกของโลหะจากตัวเร่งปฏิกิริยา เมื่อเปรียบเทียบระหว่าง Mg(Al)LaO และ รีไฮเดรท Mg(Al)La ไฮโดรเทลไชต์ ผลการทดลองบ่งชี้ว่าตัวเร่งปฏิกิริยาที่ผ่านการรีไฮเดรทแล้ว แสดงค่าการเปลี่ยนรูปของกลีเซอรอลโทรมิวทิเรตที่สูงกว่า และมีการหลุดออกของโลหะจากตัวเร่งปฏิกิริยาน้อยกว่า ได้เลือกน้ำมันรำข้าวดิบที่มีกรดไขมันอิสระสูง (11.14% FFA) มาทำปฏิกิริยาเอสเทอร์ฟิเคชันและทรานส์เอสเทอร์ฟิเคชันกับเมทานอล ได้สังเคราะห์ชุดของตัวเร่งปฏิกิริยาที่มี 15-80% ทั้งสโตฟอสฟอริกแอซิด (HPW) บนซิลิกาและพิสูจน์เอกลักษณ์ด้วย XRD, TPD และ FT-IR ได้ทำการวัดประสิทธิภาพของตัวเร่งปฏิกิริยาในการเปลี่ยนรูปของกรดไขมันอิสระ ตัวเร่งปฏิกิริยา 80 wt% HPW/SiO₂ สามารถลดกรดไขมันอิสระลงเหลือน้อยกว่า 1 เปอร์เซ็นต์ เมื่อทำปฏิกิริยาที่อุณหภูมิ 70 องศาเซลเซียส เป็นเวลา 4 ชั่วโมง และอัตราส่วนโดยโมลเมทานอลต่อน้ำมัน = 10 โดยใช้ตัวเร่งปฏิกิริยา 3 เปอร์เซ็นต์โดยน้ำหนัก หลังจากนั้นนำมาทำปฏิกิริยาทรานส์เอสเทอร์ฟิเคชันด้วยตัวเร่งปฏิกิริยารีไฮเดรท Mg(Al)La ไฮโดรเทลไชต์ ที่อุณหภูมิ 100 องศาเซลเซียส เป็นเวลา 9 ชั่วโมงด้วยอัตราส่วนของเมทานอลต่อ น้ำมัน = 30 และใช้ปริมาณตัวเร่งปฏิกิริยา 7.5 เปอร์เซ็นต์โดยน้ำหนัก ได้ไบโอดีเซลที่มีเมทิลเอสเทอร์ร้อยละ 100 และได้ผลิตภัณฑ์เท่ากับร้อยละ 75

สาขาวิชา ปิโตรเคมีและวิทยาศาสตร์พอลิเมอร์ ลายมือชื่อนิสิต...พัชรภรณ์...ช่วยปลอด.....
ปีการศึกษา.....2550..... ลายมือชื่ออาจารย์ที่ปรึกษา.....วิมลรัตน์.....

4972407623 : MAJOR PETROCHEMISTRY AND POLYMER SCIENCE

KEYWORD: HYDROTALCITE / BIODIESEL / CATALYAT / BASE / FREE FATTY ACID

PATCHARAPORN CHUAYPLOD : HETEROGENEOUS CATALYSTS FOR
BIODIESEL PRODUCTION FROM HIGH FREE FATTY ACID VEGETABLE OIL.

THESIS ADVISOR: ASSOC. PROF. WIMONRAT TRAKARNPRUK, Ph.D, 84 pp.

A two-step catalyzed process consisting of esterification and transesterification reactions was employed for the efficient conversion of rice bran oil into fatty acid methyl ester (biodiesel) using acid and base catalysts. First, the heterogeneous base catalysts: MgAl hydrotalcites (Mg/Al molar ratio = 3 and 4), metal loaded on calcined MgAl hydrotalcites: M loaded MgAlO (M = K, Cs, Sr, Ba, La) as well as Mg(Al)La hydrotalcites, Mg(Al)LaO and rehydrated Mg(Al)La were synthesized and characterized by ICP, XRD, SEM, BET and FT-IR. Their basicity was measured by titration. To compare their catalytic activity, glyceryl tributyrate was used as a model compound for transesterification with methanol. The results indicated that among metal loaded mixed oxide, 1.5 wt% K loaded on MgAlO gave the highest conversion, however, metal leaching was also detected. Comparison between Mg(Al)LaO and rehydrated Mg(Al)La hydrotalcite, the results indicated that the rehydrated catalyst exhibited higher activity and less metal leaching. Crude rice bran oil having high free fatty acids (11.14%FFA) was chosen for the esterification and transesterification reactions with methanol. The series of the solid acid catalyst containing 15-80% of 12-tungstophosphoric acid (HPW) supported onto silica were synthesized and characterized by XRD, TPD and FT-IR. The activities of the acid catalysts on the conversion of FFA were determined. FFA can be reduced to less than 1.0% using 80 wt% HPW/SiO₂ catalyst when reaction was carried out at 70°C for 4 h using a 10:1 molar ratio of methanol to oil and a catalyst amount of 3 wt%. Then, the base catalyzed transesterification using the rehydrated MgAlLa hydrotalcite (La low) catalyst was performed at 100°C for 9 h with a 30:1 molar ratio of methanol to oil and a catalyst amount of 7.5 wt% to obtain biodiesel with 100% methyl ester content and 75% product yield.

Field of study Petrochemistry and Polymer Science. Student's signature.....

Academic year.....2007..... Advisor's signature.....

ACKNOWLEDGEMENTS

The author wishes to express highest appreciation to her thesis advisor, Associate Professor Dr. Wimonrat Trakarnpruk, for her suggestions, assistance, encouragement, kindness and especially sincere forgiveness for her harsh mistakes throughout her study. She would like to thank the members of her thesis committee, Associate Professor Dr. Sirirat Kokpol, Professor Dr. Padet Sidisunthorn, Assistant Professor Dr. Worawan Bhanthumnavin, and Dr. Amarawan Intasiri as chairman and committees for their valuable discussion and advice.

She would like to thank Program of Petrochemistry and Polymer Science and Department of Chemistry, Faculty of Science, Chulalongkorn University for the instruments. She thanks the staffs of the Technological Research Equipment Center, Chulalongkorn University for sample analysis. Acknowledgement also goes to Thai Edible Oil Co., Ltd. for providing crude rice bran oil. This work is financially supported by Graduate School, Chulalongkorn University and Energy Research Institute, Chulalongkorn University.

Finally, she would like to express her deepest gratitude to her family for their kindness, encouragement and support throughout the course of her study. Moreover, she thanks her friends for their friendship and help during her graduate study.

สถาบันวิทยบริการ
จุฬาลงกรณ์มหาวิทยาลัย

CONTENTS

	Page
ABSTRACT IN THAI	iv
ABSTRACT IN ENGLISH	v
ACKNOWLEDGMENTS	vi
CONTENTS	vii
LIST OF TABLES	xi
LIST OF FIGURES	xiii
LIST OF SCHEMES	xv
LIST OF ABBREVIATIONS	xvi
CHAPTER I INTRODUCTION	1
1.1 The objectives of the thesis.....	2
CHAPTER II THEORY AND LITERATURE REVIEWS	3
2.1 Diesel fuels.....	3
2.2 Biodiesel.....	4
2.3 Catalysts.....	4
2.3.1 Homogeneous catalysts.....	4
2.3.2 Heterogeneous catalysts.....	5
2.4 Heteropolyacid (HPAs)	5
2.5 Hydrotalcites	6
2.6 Glycerol	7
2.7 Rice bran oil	8
2.8 Transesterification reaction.....	9
2.8.1 Effect of moisture and free fatty acid.....	10
2.8.2 Effect of alcohol/oil molar ratio.....	11
2.8.3 Effect of reaction time.....	11
2.8.4 Effect of reaction temperature.....	11
2.9 Literature reviews.....	11

CHAPTER III EXPERIMENTAL	18
3.1 Chemicals.....	18
3.2 Equipments.....	19
3.3 Characterization of catalysts.....	19
3.3.1 Metal content in catalysts.....	19
3.3.2 Structure and the composition of the materials.....	19
3.3.3 Surface area and porosity of catalysts.....	19
3.3.4 Functional group of catalysts	20
3.3.5 Soluble basicity of catalysts.....	20
3.3.6 Acidity properties of catalysts	20
3.4 Determination of product.....	21
3.4.1 Calculation of methyl esters product	22
3.5 Catalyst preparation.....	22
3.5.1 Acid catalyst: supported heteropolyacid	22
3.5.2 Base catalyst	23
3.5.2.1 Preparation of MgAl hydrotalcites.....	23
A. Alkali-free co-precipitation method	23
B. Alkali co-precipitation method	23
3.5.2.2 Metal loaded catalysts	23
3.5.2.3 Preparation of calcined and rehydrated Mg(Al)La hydrotalcites.....	24
3.5.2.4 Test of metal leaching from catalyst	24
3.5.2.5 Reusability of catalyst	24
3.6 Treatment of crude rice bran oil.....	25
3.6.1 Water degumming of crude rice bran oil.....	25
3.6.2 Free fatty acid measurement.....	25
3.7 Catalytic activity	25
3.7.1 Transesterification of glyceryl tributyrates	25
3.7.2 Esterification of free fatty acid in crude rice bran oil	26
3.7.3 Transesterification of treated rice bran oil	26

4.4	Crude rice bran oil	60
4.4.1	Fatty acid composition of crude rice bran oil.....	60
4.4.2	Acid-catalyzed esterification of crude rice bran oil.....	61
4.4.3	Influence of reaction parameters on esterification of FFA.....	62
	A. Effect of reaction temperature.....	62
	B. Effect of amount of catalyst	63
	C. Effect of reaction time.....	63
4.5	Base catalyzed transesterification of treated rice bran oil	64
	A Effect of methanol to oil molar ratio	65
	B Effect of catalyst amount.....	66
4.6	Proposed mechanism	67
4.7	Comparison with other works	68
CHAPTER V CONCLUSION AND SUGGESTIONS.....		69
REFERENCES.....		71
APPENDICES.....		76
VITAE.....		84

LIST OF TABLES

		Page
Table 2.1	Typical ranges of diesel engines.....	3
Table 2.2	Composition of crude rice bran oil.....	8
Table 3.1	Chemicals and suppliers	18
Table 4.1	The nominal and measured Mg/Al molar ratio.....	30
Table 4.2	Plane spacings of MgAl hydrotalcites (Mg/Al molar ratio 3)	31
Table 4.3	Unit cell dimensions of hydrotalcites (Mg/Al molar ratio 3)	32
Table 4.4	Plane spacings of MgAl hydrotalcites molar ratio 3 and 4.....	34
Table 4.5	Unit cell dimensions of MgAl hydrotalcites molar ratio 3 and 4.....	34
Table 4.6	Plane spacings of MgAlO (Mg/Al molar ratio 4).....	35
Table 4.7	Unit cell dimensions of MgAlO comparison with other work.....	35
Table 4.8	Textural properties of MgAlO catalysts.....	38
Table 4.9	Textural properties of metal loaded mixed oxide catalysts.....	40
Table 4.10	Soluble basicity of catalysts.....	42
Table 4.11	Lattice parameters of MgAlLa hydrotalcites and Mg(Al)LaO.....	44
Table 4.12	The metal content of Mg(Al)LaO catalyst.....	45
Table 4.13	Textural properties of Mg(Al)LaO catalysts.....	47
Table 4.14	Textural properties of rehydrated Mg(Al)La hydrotalcite catalysts.....	48
Table 4.15	Soluble basicity of La containing catalysts.....	49
Table 4.16	Glycerol tributyrated conversion using MgAlO catalysts.....	50
Table 4.17	Transesterification of glycerol tributyrate using Mg(Al)LaO and rehydrated Mg(Al)La hydrotalcites.....	53
Table 4.18	The soluble basicity of recovered and fresh catalyst.....	55
Table 4.19	Textural properties of SiO ₂ and HPW/SiO ₂	58
Table 4.20	The total acidity of HPW and HPW/SiO ₂	59
Table 4.21	Composition of crude rice bran oil.....	60
Table 4.22	The remaining free fatty acid after esterification reaction.....	61
Table 4.23	Transesterification of treated rice bran oil as a function of methanol/oil molar ratio.....	65

Table 4.24	Transesterification of treated rice bran oil as a function of catalyst amount.....	66
Table 4.25	Comparison of the result from this work with other works	67



สถาบันวิทยบริการ
จุฬาลงกรณ์มหาวิทยาลัย

LIST OF FIGURES

	Page
Figure 2.1 Heteropolyacid structure.....	6
Figure 2.2 Schematic representation of the hydrotalcites anionic clay structure.....	7
Figure 2.3 Synthesis of biodiesel via two step catalyzed process.....	9
Figure 2.4 The transesterification reaction of vegetable oil with alcohol to ester and glycerol.....	10
Figure 4.1 The chart of synthesized catalysts.....	29
Figure 4.2 XRD Patterns of MgAl hydrotalcites (Mg/Al molar ratio 3).....	31
Figure 4.3 XRD Patterns of MgAl hydrotalcites molar ratio 3 at pH 8 and 11.....	33
Figure 4.4 XRD Patterns of MgAl hydrotalcites molar ratio =3 and 4.....	33
Figure 4.5 XRD Patterns of MgAlO (Mg/Al molar ratio 4) compared with MgAl hydrotalcite.....	35
Figure 4.6 XRD Patterns of MgAl oxide loaded with different metal.....	36
Figure 4.7 SEM images ($\times 20,000$ magnification) of (A) MgAl hydrotalcites.....	37
(B) 1.5%K mixed oxide	37
Figure 4.8 N ₂ adsorption-desorption isotherm of MgAlO	38
Figure 4.9 N ₂ adsorption-desorption isotherm of metal loaded mixed oxide.....	39
Figure 4.10 FT-IR spectra of (A) MgAl hydrotalcite, (B) MgAlO and (C) 1.5wt%K MgAlO.....	41
Figure 4.11 XRD Patterns of Mg(Al)La hydrotalcites and the Mg(Al)LaO.....	43
Figure 4.12 XRD Patterns of Mg(Al)LaO and the rehydrated Mg(Al)La hydrotalcites.....	44
Figure 4.13 SEM images ($\times 20,000$ magnification) of (A) Mg(Al)LaO.....	46
(B) Rehydrated Mg(Al)La hydrotalcites.....	46
Figure 4.14 N ₂ adsorption-desorption isotherm of Mg(Al)LaO	47
Figure 4.15 Catalytic activities of K-MgAlO with different amount of metal and ratio.....	51

Figure 4.16	Catalytic activity of 1.5% wt metal loading with different metal and Mg/Al molar ratios.....	52
Figure 4.17	Catalytic activities of fresh catalyst and recovered catalyst	54
Figure 4.18	XRD Patterns of HPW and HPW/SiO ₂	56
Figure 4.19	N ₂ adsorption-desorption isotherm of (A) non loaded mesoporous silica.....	57
	(B) HPW loaded mesoporous silica.....	57
Figure 4.20	NH ₃ -TPD of HPW and HPW/silica.....	58
Figure 4.21	FTIR spectra of HPW and HPW/SiO ₂	59
Figure 4.22	Remaining FFA as a function of reaction temperature.....	62
Figure 4.23	Remaining FFA as a function of amount of catalyst.....	63
Figure 4.24	Remaining FFA as a function of reaction time.....	64
Figure A-1	Gas chromatogram of liquid product from reaction mixture of transesterification of glyceryl tributyrate.....	77
Figure A-2	Gas chromatogram of liquid mixture for correction factor calculation.....	78
Figure A-3	Gas chromatogram of liquid product from reaction mixture of transesterification of glyceryl tributyrate using 1.5 wt% MgAlO catalyst..	80
Figure A-4	Gas chromatogram of products from crude rice bran teansesterification....	82

LIST OF SCHEMES

	Page
Scheme 1 Mechanism of base-catalyzed transesterification of oil.....	67



สถาบันวิทยบริการ
จุฬาลงกรณ์มหาวิทยาลัย

LIST OF ABBREVIATIONS

ADS	adsorption
atm	atmosphere
BET	Brunauer-Emmett-Teller method
deg	degree
DES	desorption
°C	degree Celsius
FT-IR	Fourier Transform Infrared spectroscopy
FFA	free fatty acid
GC	gas chromatography
g	gram (s)
h	hour (s)
HT	hydrotalcite
ICP	Inductively Coupled Plasma Emission
IUPAC	International Union of Pure and Applied Chemistry
MeOH	methanol
mmol	millimole
ml	milliliter (s)
min	minute
SEM	Scanning Electron Microscopy
sec	second
TPD	Temperature-programmed desorption
HPW	12-tungstophosphoric acid
cm ⁻¹	unit of wavenumber
XRD	X-ray diffraction

CHAPTER I

INTRODUCTION

Due to the predicted shortness of conventional fuels and environmental concerns, a search for alternative fuels has gained recent significant attention. As the calorific value of vegetable oil is comparable to that of diesel, they could be used as fuel in compression ignition engines. The demand for diesel fuel in Thailand is about 43 million liters per day of diesel, which was 46.6 % of total consumption of petroleum product [1]. The consumption of diesel fuel in Thailand is being continuously increased. The increasing demand for energy has prompted a lot of research to produce alternative fuels from renewable resources. Alternative fuels should be easily available, environmental friendly and technoeconomically competitive.

Biodiesel produced by transesterification reactions can be alkali catalyzed, acid catalyzed or enzyme catalyzed. Only well refined vegetable oil with less than 1.0 wt% free fatty acid (FFA) can be used as the reactant in this process. When crude oil with more than 1.0 wt% FFA is used, an acid catalyzed process is preferred. Hence, a combined process with acid catalyzed pretreatment was developed to synthesize biodiesel from high free fatty acid vegetable oil. The first step is to esterify the FFA with methanol by acid catalysis. When the FFA content is lower than 1.0 wt% then the alkali is introduced into the system to complete the transesterification [2].

Transesterification is performed using homogeneous acid or base catalyst. Base catalyst is preferred to acid catalyst routes. The main disadvantage of this method is the formation of soaps due to the reaction of the alkaline catalysts with free fatty acids, or due to saponification of the triglycerides and biodiesel. These reactions consume the catalyst and hinder phase separation of the biodiesel product from the glycerol side-product, which in practice results in decrease yield. A further disadvantage is that the glycerol by product contains salts from the neutralization of the catalyst [3].

Therefore, conventional homogeneous catalysts are expected to be replaced in the near future by environmentally friendly heterogeneous catalysts mainly because of environmental constraint and simplification in the existing processes. Heterogeneous catalyst leaves no neutralization salts in the glycerol by-product, and, as the catalyst is not continuously added and disposed of, the inputs and waste is reduced. The catalyst can also be retained in the reactor by a simple filtration, and does not need to be neutralized to quench the reaction as in conventional technology. More recent research has focused on the use of heterogeneous catalysts [4].

Although solid base, such as clays, zeolites, alumina oxides, were widely explored, the reaction temperature seemed to be high. Hydrotalcites $[M^{2+}_{(1-x)} M^{3+}_x (OH)_2]^{x+} (A_{x/n})^{n-} \cdot yH_2O$ were interesting basic materials. It was reported to give higher yields in transesterification reaction. Its acid/basic properties could be easily controlled by varying their composition [5]. Hydrotalcites have been used as precursors of catalyst and have attracted much attention during the development of new environmentally friendly catalyst.

1.1 Objectives of the research

- To synthesize and characterize metal loaded catalysts from calcined MgAl hydrotalcites and Mg(Al)La hydrotalcites.
- To study the reaction parameters affecting catalytic activity of the synthesized catalysts in transesterification of glyceryl tributyrates (as a model compound of vegetable oil) with methanol.
- To study two steps catalysis: acid-catalyzed esterification and base-catalyzed transesterification of crude rice bran oil with methanol utilizing the suitable catalyst.

CHAPTER II

THEORY AND LITERATURE REVIEWS

2.1 Diesel fuels

There are three basic types of diesel fuels:

High-speed diesel is normally used as a fuel for high-speed diesel engines operating above 1,000 rpm such as trucks, cars, buses, locomotives, and pumping sets *etc.* Gas turbine requiring distillate fuels normally make use of high-speed diesel as fuel.

Medium-speed diesel is used for a wide range of purpose including generation of electricity, stationary power generators, railroads, and pipeline pumps. It operates range of 450 to 1,000 rpm.

Low-speed diesel or marine diesel is commonly used on ships. Fishing boats, and for generation of electricity. Low-speed diesel can operate below 300 rpm. Typical ranges of diesel engines are listed at Table 2.1

Table 2.1 Typical ranges of diesel engines

Type	Speed Range	Conditions	Typing application
Low Speed	<300 rpm	Heavy load, constant speed	Marine main propulsion; electric power generation
Medium Speed	300-1000 rpm	Fairy high load Relatively constant speed	Marine auxiliaries; Stationary power
High Speed	>1000 rpm	Frequent and wide variation in load and speed	Generators; pumping units Road transport vehicles; diesel locomotives

2.2 Biodiesel

Biodiesel produced from vegetable oil or animal fat including waste cooking oil. Biodiesel is used in diesel engine without modification because it has properties similar to petroleum diesel fuel. Biodiesel has a superior lubricity, high flash point and cetane number, high oxygen content, low poison, as well as high biodegradability. Moreover, it is essentially free sulfur and the engines fueled by biodiesel emit significantly fewer particulate matters, unburnt hydrocarbons and less carbon monoxide than operating on conventional fossil fuels [6].

A variety of oils can be used to produce biodiesel. These include:

- Virgin oil feedstock

Rapeseed, palm oil and soybean oils are most commonly used, soybean oil alone accounting for about ninety percent of all fuel stocks.

- Waste vegetable oil

- Animal fats

Tallow, lard, yellow grease, chicken fat.

2.3 Catalysts

Biodiesel can be produced using alkali catalyzed, acid catalyzed or enzyme catalyzed, but the first two types have received more attention because of the short reaction times and low cost compared with the third one. It can be produced using either homogeneous catalyst or heterogeneous catalyst.

2.3.1 Homogeneous catalysts

Alkaline metal alkoxides are the most active catalysts, since they give very high yield (> 98%) in short reaction time (30 min) even if they are applied at to low concentrations (0.5 mol%). However, they require the absence of water which makes them inappropriate for typical industrial processes. Alkaline metal hydroxides (KOH and

NaOH) are cheaper than metal alkoxides, but less active. However, even if a water-free alcohol/oil mixture is used, some water is produced in the reaction of the produced ester, with consequent soap formation. This undesirable saponification reaction reduces the ester yields and considerably disturbs the recovery of the glycerol due to the formation of emulsions. Potassium carbonate, used in concentration of 2 or 3 mol%, give high yields of fatty acid alkyl esters and reduces the soap formation. This can be explained by the formation of bicarbonate instead of water, which does not hydrolyse ester.

2.3.2 Heterogeneous catalysts

Heterogeneous catalysts can be easily separated from the reaction mixture without any solvent, and show easy regeneration and have a less corrosive character, leading to safer, cheaper and more environment-friendly operation. Because of the presence of heterogeneous catalysts, the reaction mixture constitutes a three-phase system, oil/methanol/catalyst, which for diffusion reasons inhibits the reaction. Nevertheless, heterogeneous catalysts could improve the synthesis methods for the development of an environmentally benign process and the reduction of production cost.

2.4 Heteropolyacid (HPAs)

The heteropolyacids are strong acids, for instance, their significantly higher Brønsted acidity, compared with the acidity of traditional mineral acid catalysts, is of great importance for catalysis. Their acid strength depends on the type of hetero atom, which one can be turned to a suitable catalyst for the acid-catalyzed reactions [7]. HPAs are very good acid catalysts in homogeneous medium. They catalyze a wide variety of reactions offering strong and cleaner processing compared to conventional mineral acid. The main disadvantages of HPAs as catalyst lie in their low thermal stability, low surface area (1-10 m²/g) and separation from reaction mixture.

Thus, the development of new solid catalyst with advanced characteristic of strength, surface area, porosity, etc. The supporting of HPAs on the suitable support is expected to overcome the mentioned problem of HPAs [8].

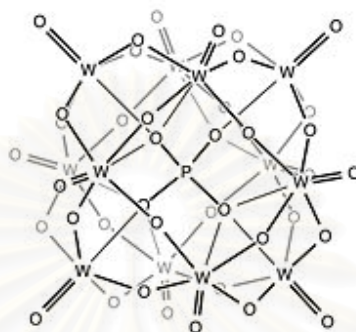


Figure 2.1 Heteropolyacid structure.

2.5 Hydrotalcites

Hydrotalcites of general formulae $[M^{2+}_{(1-x)}M^{3+}_x(OH)_2]^{x+}(A_{x/n})^{n-} \cdot yH_2O$ are another interesting class of solid base whose acid/basic properties can be easily controlled by varying their composition. The structure of hydrotalcites is based upon layered double hydroxides with brucite like $(Mg(OH)_2)$ hydroxide layers containing octahedrally coordinated M^{2+} and M^{3+} cations. A^{n-} is the counter anion which resides in the interlayer space to balance the residual positive charge of the hydroxide layers which results from isomorphous substitution of M^{2+} by M^{3+} . Variations in the Al content (x) are known to modify the basic properties of the material, with stable pure hydrotalcite structures reported to form for compositions over the range $0.25 < x < 0.44$. Outside of these limits the high density of Mg^{2+} or Al^{3+} octahedral will lead to the formation of $Mg(OH)_2$ and $Al(OH)_3$ respectively.

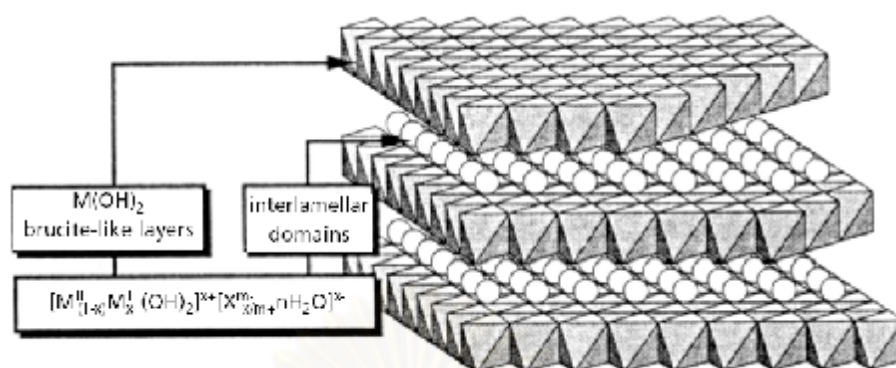


Figure 2.2 Schematic representation of the hydrotalcite anionic clay structure [9].

Mixed oxides are obtained after calcination performed in the temperature range of 450-500°C. In hydrotalcite, physisorbed and interstitial water are removed at temperatures above ~100°C and ~187°C, respectively. At more elevated temperatures (above 250°C) the hydrotalcite undergoes dehydroxylation and decarboxylation via H₂O and CO₂ evolution, giving rise to an increased surface area and formation of mesopores. Thus, calcination at high temperature decomposes the hydrotalcite into mixed Mg-Al oxides. The basic sites in the alkali earth oxides component can originate from O²⁻ (strong basicity), O⁻ species near hydroxyl groups (medium strength) and OH groups (weak). The addition of Al³⁺ alters the acid:base site distribution through the introduction of Al³⁺-O²⁻ sites which are of moderate Lewis acidity and only medium basicity [10].

2.6 Glycerol

Glycerin or 1, 2, 3,-propanetriol propantriol, CH₂OHCHOHCH₂OH, is colorless, odorless, sweet-tasting, syrupy trihydric alcohol. It melts at 17.8°C; boils with decomposition at 290°C. It is miscible with water and ethanol. It is hygroscopic; this property makes it valuable as moistener in cosmetics. It is present in the form of its ester (glycerides) in all animal and vegetable fats and oils and obtained commercially as byproduct when fats and oils are hydrolyzed to yield fatty acids or their metal salts (soaps). In addition, it is widely used as a solvent; as a sweetener; in the manufacture of

dynamite, cosmetics, liquid soaps, candy, liqueurs, inks, and lubricants; to keep fabrics pliable; as a component of antifreeze mixture; as a source of nutrients for fermentation cultures in the production of antibiotics; and in medicine.

2.7 Rice bran oil

Rice bran oil (RBO) offers significant potential as an alternative low-cost feedstock for biodiesel production. Rice bran has great potential as a supplementary source of many nutrients. Recent findings show that rice bran in reducing serum cholesterol and reducing the risk of heart disease.

Rice bran oil is one of the most nutritious oils due to its favorable fatty acid composition and a unique combination of naturally occurring biologically active and antioxidant compounds, such as γ -oryzanol, vitamin E, phytosterols, and tocotrienols. In addition, rice bran also contains high molecular weight wax esters, which is a source of policosanols [11]. Crude RBO has been difficult to refine because of its high content of free fatty acid, unsaponifiable matter and dark color. Lists the fatty acid composition of crude RBO are shown in Table 2.2.

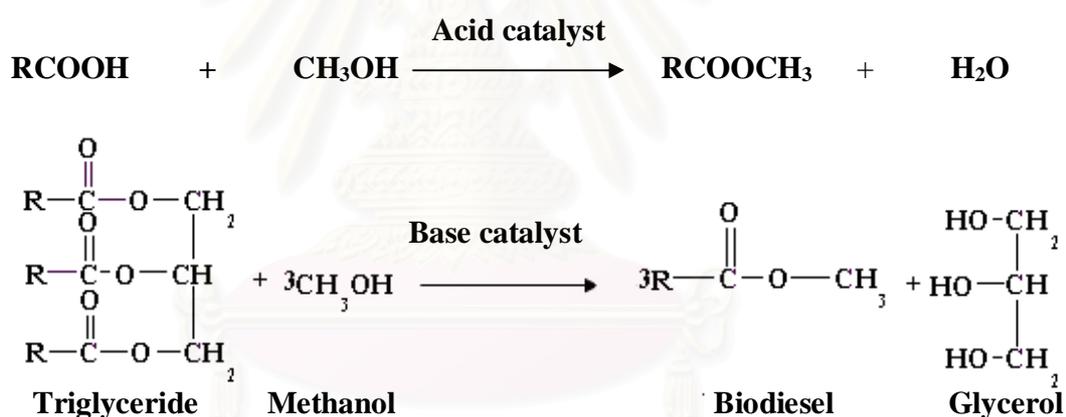
Table 2.2 Composition of crude rice bran oil

Fatty acid	(%)
C16:0 Palmitic acid	18.3
C18:0 Stearic acid	2.4
C18:1 Oleic acid	41.4
C18:2 Linoleic acid	37.9

2.8 Transesterification reaction

Transesterification reaction can be alkali catalyzed, acid catalyzed or enzyme catalyzed. An alkali catalyzed process can achieve high purity and yield of biodiesel product in a short time. However, it is very sensitive to the purity of the reactants. Only well refined vegetable oil with less than 1 wt% free fatty (FFA) can be used as the reactant in this process.

Hence, a combined process with acid catalyzed pretreatment was developed to synthesize biodiesel from high free fatty acid vegetable oil. The first step is to esterify the FFA with methanol by acid catalysis. When the FFA content is lower than 1 wt% the alkali is introduced into the system to complete the transesterification.



where R is long hydrocarbon chains, sometimes called fatty acid chains.

Figure 2.3 Synthesis of biodiesel via two step catalyzed process.

Transesterifications consist of a number of consecutive, reversible reactions [12]. The triglyceride is converted stepwise to diglyceride, monoglyceride and finally glycerol (Fig. 2.3). A mole of ester is liberated at each step. The reactions are reversible, although the equilibrium lies towards the production of fatty acid esters and glycerol.

The reaction mechanism for alkali-catalyzed transesterification was formulated as three steps. The first step is an attack on the carbonyl carbon atom of triglyceride molecule by the anion of the alcohol (methoxide ion) to form a tetrahedral intermediate react with an alcohol (methanol) to regenerate the anion of the alcohol (methoxide ion). In the last step, rearrangement of the tetrahedral intermediate result in the formation of a fatty acid ester and diglyceride. A small amount of water, generated in the reaction, may cause soap formation during transesterification.

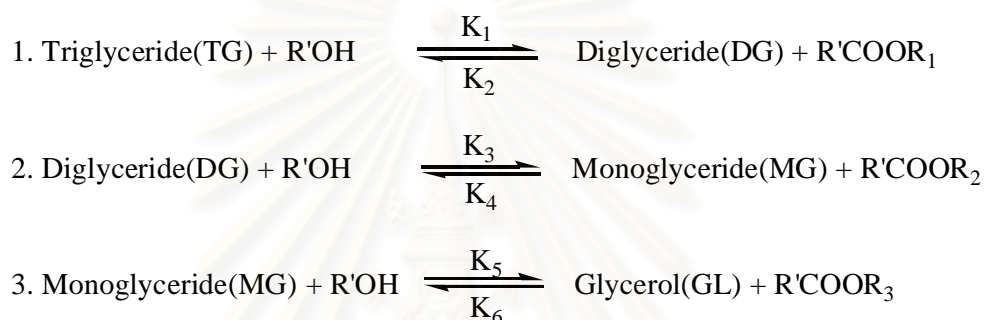


Figure 2.4 The transesterification reactions of vegetable oil with alcohol to esters and glycerol [13].

Parameters influencing the transesterification have been studied, and can be concluded as follows:

2.8.1 Effect of moisture and free fatty acid

The glycerides should have an acid value less than 1.0%wt and all materials should be substantially anhydrous. If the acid value was greater than 1.0%wt, more NaOH was required to neutralize the free fatty acids. Water also caused soap formation, which consumed the catalyst and reduced catalyst efficiency. The resulting soap caused and increased in viscosity, formation of gels and made the separation of glycerol difficult [14].

2.8.2 Effect of alcohol/oil molar ratio

The stoichiometric ratio for transesterification requires three moles of alcohol and one mol of glyceride to yield three moles of fatty acids ester and one mole of glycerol. An acid catalyzed reaction needed a 30:1 alcohol/ oil ratio, while an alkali-catalyzed reaction required only a 6:1 ratio to achieve the same ester yield for a given reaction time [12].

2.8.3 Effect of reaction time

The conversion rate increases with reaction time [12]. The reaction was initially very slow due to the mixing and dispersion of methanol into oil. Later on, the reaction proceeded very fast and reached the maximum value.

2.8.4 Effect of reaction temperature

Transesterification can occur at different temperatures, depending on the oil used. It can be room temperature or high temperature.

2.9 Literature reviews

One step catalysis

Homogeneous catalysts

In 2001 Kuadiana *et al.* prepared methyl esters from rapeseed oil by supercritical method. Effects of reaction temperature, reaction pressure and molar ratio of methanol to triglycerides were investigated. The results revealed that the supercritical treatment of 350°C, 30 MPa and 240 sec with molar ratio of 42 was the best condition for transesterification [15].

In 2003 Tomasevic *et al.* performed transesterification reaction of refined sunflower oil and used frying oils at 25°C with homogeneous catalysts: potassium hydroxide or sodium hydroxide. Reaction parameters studied included oil quality, molar ratio of methanol to oil, type and catalyst concentration, temperature and reaction time. With 1% potassium hydroxide, temperature at 25°C, molar ratio of methanol to oil = 6:1 and reaction time of 30 min, all oils were sufficiently transesterified and could be used as fuel in diesel engines [16].

In 2005, Felizardo *et al.* studied transesterification of waste frying oils with methanol using sodium hydroxide as catalyst. Methanol/oil molar ratios and catalyst/oil weight ratios were varied. For oils with an acid value of 0.42 mg KOH/g, the results showed that a methanol/oil ratio of 4.8 and a catalyst 0.6% gave the highest yield of methyl esters in 1 h reaction time. Furthermore, an increase in the amount of methanol or catalyst quantity seems to simplify the separation/purification of the methyl esters phase, as shown by a viscosity reduction and an increasing purity to values higher than 98% for methyl esters phase [17].

Heterogeneous catalysts

In 2000, Choundary *et al.* studied transesterification of normal and β -ketoesters with primary, secondary, unsaturated, allylic, cyclic, hindered alcohols and amines using Mg–Al–O–*t*-Bu hydrotalcite catalyst. The catalyst showed 98% yield for the transesterification of methyl acetoacetate and 1-hexanol at 90 °C for 2 h, using 10 ml toluene as a solvent. This catalyst can be reused 6 times without loss of activity [18].

In 2004, Kim *et al.* studied transesterification of vegetable oils using Na/NaOH/ γ -Al₂O₃ heterogeneous catalyst which was prepared by loading 20 wt% of sodium hydroxide and 20 wt% sodium metal onto the alumina support in nitrogen atmosphere. The reaction conditions were optimized and found to be 1 h reaction time, the stirring speed of 300 rpm, *n*-hexane was used as co-solvent, the methanol to oil molar ratio =

9:1. The maximum yield reached 94%, which was close to the conventional homogeneous NaOH catalyst system [19].

In 2005, Furuta *et al.* evaluated amorphous zirconia, titanium-, aluminum-, and potassium-doped zirconia in the transesterification of soybean oil with methanol at 250°C, and the esterification of *n*-octanoic acid with methanol at 175–200°C. Titanium- and aluminum-doped zirconia showed high performance, with over 95% conversion in both esterifications [20].

In 2005, Cantrell *et al.* synthesized a series of $[\text{Mg}_{(1-x)}\text{Al}_x(\text{OH})_2]^{x+}(\text{CO}_3)_{x/n}^{2-}$ hydrotalcite materials with compositions over the range $x = 0.25\text{--}0.55$ using an alkali-free co-precipitation method. All materials exhibited XRD patterns characteristic of the hydrotalcite phase with a steady lattice expansion observed with increasing Mg content. All materials are effective catalysts for the liquid phase transesterification of glyceryl tributyrate with methanol for biodiesel production. The rate increases steadily with Mg content. This catalyst is more active than MgO [10].

In 2005, Birjega *et al.* prepared rare-earth elements (REE) species in hydrotalcite structures to be used as catalysts for basic catalyzed organic reactions. The rare earth-elements chosen for the study were Y^{3+} , Dy^{3+} , Gd^{3+} , Sm^{3+} , La^{3+} . Their derived mixed oxides were obtained by the thermal decomposition of hydrotalcite at 460°C for 18 h under argon flow. They are very active and selective in the reaction of cyanoethylation of ethanol with acrylonitrile [21].

In 2005, Sepulveda *et al.* prepared and characterized tungstophosphoric acid (HPA) catalysts supported over SiO_2 and ZrO_2 in the liquid phase esterification of acetic acid with butanol. The results revealed that silica- and zirconia supported HPA catalysts had an intrinsic activity per unit protonic acid site greater than that of an Amberlyst W35 resin. Its repeated use was, however, impeded because of the dissolution of HPA in the reaction medium. Meanwhile carbon-supported HPA catalysts had a slightly lower

activity but they displayed a sustained conversion level upon reuse in subsequent catalytic tests [22].

In 2005, Arabi *et al.* studied esterification of phthalic anhydride with 2-ethylhexanol and 1-butanol. They also studied ester decomposition of dioctyl phthalate (DOP) in presence of Keggin type heteropolyacids; $H_3PW_{12}O_{40}$, $H_4SiW_{12}O_{40}$, $H_4SiMo_{12}O_{40}$, Wells–Dawson type heteropolyacids; $H_6P_2W_{18}O_{62}$, $H_6P_2W_{17}MoO_{62}$ and Preyssler type heteropolyacids; $H_{14}[NaP_5W_{29}MoO_{110}]$, $H_{14}[NaP_5W_{30}O_{110}]$. The Preyssler and Wells–Dawson types and their molybdenum substituted derivatives show higher activity in esterification and ester decomposition reactions than the Keggin type heteropolyacids [7].

In 2006, Huaping *et al.* produced biodiesel by the transesterification of jatropha curcas oil using a heterogeneous solid superbase catalyst: calcium oxide. The results showed that the base strength of calcium oxide was more than 26.5 after dipping in an ammonium carbonate solution followed by calcination. At catalyst calcination temperature of 900°C , reaction temperature of 70°C , reaction time of 2.5 h, catalyst dosage of 1.5%, and methanol/oil molar ratio of 9:1, the oil conversion was 93% [23].

In 2006, Xie *et al.* studied the methanolysis of soybean oil to methyl esters using calcined Mg–Al hydrotalcites as solid base catalysts. When the reaction was carried out at reflux of methanol, with a molar ratio of soybean oil to methanol of 15:1, a reaction time 9 h and a catalyst amount 7.5%, the oil conversion was 67%. The calcined hydrotalcite with an Mg/Al ratio of 3 and with calcination at 500°C was found to give the highest basicity and the best catalytic activity [24].

In 2007, Liu *et al.* studied transesterification of soybean oil to biodiesel using SrO as a solid base catalyst. The results showed that the yield of biodiesel was 95% at temperatures 70°C within 30 min. The catalyst had a long lifetime and could maintain activity even after 10 cycles use [25].

In 2007, Xie *et al.* performed transesterification of soybean oil with methanol to methyl esters using NaX zeolites loaded with KOH as a catalyst. Best result was obtained with NaX zeolite loaded with 10% KOH, followed by heating at 120°C for 3 h. When the transesterification reaction was carried out at reflux of methanol (65°C), with a 10:1 molar ratio of methanol to soybean oil, a reaction time of 8 h and a catalyst amount of 3 wt%, the conversion of soybean oil was 85.6% [26].

In 2007, Yang and Xia used alkaline earth metal-doped zinc oxide as a heterogeneous catalyst for transesterification of soybean oil. The ZnO was loaded with 2.5 mmol Sr(NO₃)₂/g ZnO, followed by calcination at 600°C for 5 h. Transesterification reaction was carried out at reflux of methanol (65°C), with a 12:1 molar ratio of methanol to soybean oil and a catalyst amount of 5 wt.%, the conversion of soybean oil was 94.7%. Besides, when using tetrahydrofuran (THF) as a co-solvent, the conversion was increased to 96.8% [27].

In 2007, MacLeod *et al.* studied a series of alkali-doped metal oxide catalysts for the transesterification of rapeseed oil to biodiesel. The catalysts include LiNO₃/CaO, NaNO₃/CaO, KNO₃/CaO and LiNO₃/MgO, they exhibited >90% conversion in 3 h test. However, metal leaching from the catalyst was detected, and this resulted in some homogeneous activity [28].

Two-step catalysis

In 2005, Zullaikah *et al.* studied the effect of temperature, moisture and storage time on the accumulation of free fatty acid in the rice barn. The result showed that free fatty acid content was raised up to 76% in six month at room temperature. A two-step acid-catalyzed process was employed to biodiesel from rice bran oil. The first step was carried out at 60°C using H₂SO₄ as catalyst and the molar ratio of methanol:FFA of 5: 1. More than 98% FFA conversion was found. Then the following step, acid-catalysis was carried out at 100°C. From two-step methanolysis reaction, more than 98% FAME in the product can be obtained [11].

In 2005, Ghadge *et al.* prepared biodiesel from mahua oil having 19% free fatty acids. The high FFA level of mahua oil was reduced to less than 1% by a two-step pretreatment process. The first step was carried out with 0.30–0.35 v/v methanol-to-oil ratio in the presence of 1% v/v H₂SO₄ as an acid catalyst in 1 h reaction time at 60°C. In the second step, the product from acid-catalyzed reaction was transesterified using 0.25 v/v methanol and 0.7% w/v KOH as an alkaline catalyst [29].

In 2005 Ramadhas *et al.* prepared biodiesel from rubber seed oil via a two-step transesterification process. In the first step, H₂SO₄ was used as catalyst for the acid-catalyzed process to reduce the FFA content of the oil to less than 2%. In the second step, alkaline catalyzed transesterification process, NaOH was used to convert the products of the first step to its mono-esters and glycerol [30].

In 2007, Berchmans *et al.* prepared biodiesel from crude *Jatropha curcas* seed oil (CJCO) having 15% FFA. The high FFA level of CJCO was reduced to less than 1% by a two-step process. The first step was carried out with 0.60 w/w methanol-to-oil ratio in the presence of 1% w/w H₂SO₄ as an acid catalyst in 1h reaction at 50 °C. The second step was carried out using 0.24 w/w methanol-to-oil and 1.4% w/w NaOH to oil as alkaline catalyst at 65 °C. The final yield for methyl esters was 90% in 2 h [31].

It can be seen from literature that most of oil with having high free fatty acid content was prepared via two-step catalyzed. The first step is acid catalyzed esterification reaction and following with base catalyzed transesterification reaction. Thus, biodiesel from crude rice bran oil having 11.14 % FFA was prepared via two-step catalyzed.

There is not much literature using calcined hydrotalcites as solid base catalyst for biodiesel production. Loading alkali salt on a porous support is an efficient way to create strong basic or superbasic materials [32]. Potassium nitrate was supported on calcined hydrotalcites, and its basicity of potassium-salt-modified hydrotalcites was found to be stronger than the calcined one [33]. Furthermore, modified hydrotalcite with rare earth element is also increase basicity of the catalyst [21]. In this work, transesterification of

glyceryl tributyrate (as model compound of vegetable oil) was performed to screen the basic metal loaded mixed oxide and hydrotalcites modified with La catalysts. The suitable catalyst is then used for transesterification crude rice bran oil after reduce the free fatty acid content by esterification reaction using supported heteropolyacid.



สถาบันวิทยบริการ
จุฬาลงกรณ์มหาวิทยาลัย

CHAPTER III

EXPERIMENTAL

3.1 Chemicals

All chemicals (analytical grade) used were obtained as follows:

Table 3.1 Chemicals and suppliers

Chemicals	Suppliers
Aluminium nitrate nonahydrate	Fluka Chemies A.G., Switzerland
Ammonium carbonate	Aldrich Chemical Company, Inc., USA
Ammonium hydroxide	Fluka Chemies A.G., Switzerland
Barium nitrate	Fluka Chemies A.G., Switzerland
Benzoic acid	Fluka Chemies A.G., Switzerland
Bromothymol blue	Fluka Chemies A.G., Switzerland
Cesium nitrate	Fluka Chemies A.G., Switzerland
Decane	Fluka Chemies A.G., Switzerland
Glyceryl tributyrate (tributylin)	Merck
Hexane	Merck
Lanthanum nitrate hexahydrate	Fluka Chemies A.G., Switzerland
Magnesium nitrate hexahydrate	Fluka Chemies A.G., Switzerland
Methanol	Merck
Methyl laurate	Merck
Phenolphthalein	Fluka Chemies A.G., Switzerland
Potassium acetate	Fluka Chemies A.G., Switzerland
Silicon oxide	Fluka Chemies A.G., Switzerland
Sodium hydroxide	Aldrich Chemical Company, Inc., USA
Sodium carbonate	Aldrich Chemical Company, Inc., USA
Strontium nitrate	Fluka Chemies A.G., Switzerland
12-Tungstophosphoric acid	Fluka Chemies A.G., Switzerland

3.2 Equipments

Inductive couple plasma emission (ICP-AES) Perkin Elmer model PLASMA-1000 was used for determination of elemental content in catalyst. Powder X-ray diffraction patterns were measured on a Rigaku, DMAX 2002/Ultima X-ray diffractometer with nickel filtered CuK_{α} radiation. The BET surface area and pore size distribution were determined by N_2 adsorption-desorption isotherm at 77 K using Quantachrome Autosorb-1 nitrogen adsorptometer. A Nicolet FT-IR Impact 410 Spectrophotometer was used for determination of functional group in catalyst. Acidity properties of catalysts were measured by temperature programmed desorption (TPD) of NH_3 by a commercial TPD system MODEL BEL-CAT equipped with a quadrupole mass spectrometer.

3.3 Characterization of catalysts

3.3.1 Metal content in catalysts

Metal content in catalyst was determined using inductive couple plasma emission (ICP-AES) Perkin Elmer model PLASMA-1000 at the Scientific and Technology Research Equipment Centre, Chulalongkorn University.

3.3.2 Structure and the composition of the materials

Structure and the composition of the crystalline material were determined by X-ray diffraction spectrometer (XRD). The XRD patterns of the catalyst were obtained using Rigaku, DMAX 2002/Ultima Plus powder X-ray diffractometer using CuK_{α} radiation, over a 2θ range of $5-70^\circ$ with step size of 0.02° at a scanning speed of $5^\circ/\text{min}$.

3.3.3 Surface area and porosity of catalysts

Surface area measurements were performed by N_2 physisorption at 77 K using BELSORP-mini. Prior to N_2 physisorption, the samples were outgassed for 3h at 400°C .

Surface areas were calculated using the BET (Brunauer-Emmett-Teller method) equation. The pore size distributions were obtained according to the Barret–Joyner–Halenda (BJH) method from the adsorption branch data.

3.3.4 Functional group of catalysts

Functional groups of catalyst were determined by Fourier-transform infrared spectra (FT-IR). The FT-IR spectra were recorded on a Nicolet FT-IR Impact 410 Spectrophotometer at the Department of Chemistry, Chulalongkorn University. The samples were made into a KBr pellet. Infrared spectra were recorded between 400 and 4000 cm^{-1} in transmittance mode.

3.3.5 Soluble basicity of catalysts

Soluble basicity of catalysts were determined by titration method as describe in [22]. Catalyst (0.4 g) was stirred in 25 mL of distilled water at room temperature for 2 h and then filtered. The filtrate was titrated with 0.02 M benzoic acid solution (in methanol). The indicator used was bromothymol blue. The soluble basicity was calculated by mmol of benzoic acid used in the titration of 1 g catalyst.

3.3.6 Acidity properties of catalysts

The acidic properties of samples were measured by temperature programmed desorption (TPD) of NH_3 by a commercial TPD system MODEL BEL-CAT equipped with a quadrupole mass spectrometer. The catalyst (0.15 g) was pretreated at 300°C in He flow for 2 h. NH_3 was flushed at 100°C for 1 h in He flow, then the sample was heated up to 700°C at a rate of 10°C min^{-1} .

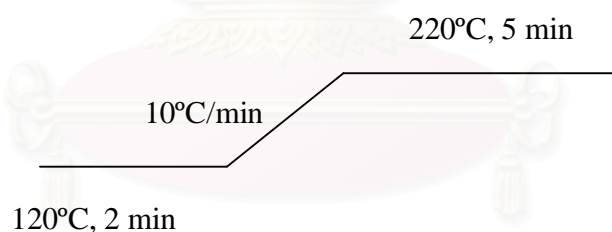
3.4 Determination of products

Reactant and products of transesterification of glyceryl tributyrates and crude rice bran oil were analyzed by gas chromatograph GC16A (Shimadzu) fitted with a DB-1 capillary column.

GC condition for the determination of conversion of glyceryl tributyrates

Column	: DB-1
Detector	: Flame ionization (FID)
Detector temperature	: 250°C
Injector temperature	: 250°C
Carrier gas	: Nitrogen
Flow rate	: 70 mL/min

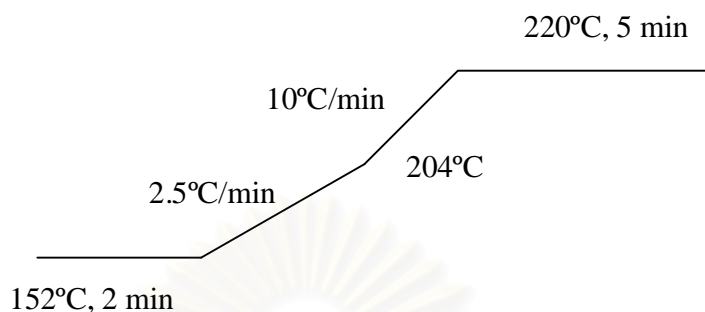
Temperature program:



GC conditions for the determination of fatty acid methyl ester

Column	: DB-1
Detector	: Flame ionization (FID)
Detector temperature	: 220°C
Injector temperature	: 220°C
Carrier gas	: Nitrogen
Flow rate	: 100 mL/min

Temperature program:



3.4.1 Calculation of methyl esters product

The analysis of methyl ester was carried out by GC.

Methyl esters content (%)

$$= \frac{(\text{weight of reference} \times \text{area of methyl esters}) \times 100}{\text{area of reference} \times \text{weight of methyl esters}}$$

Product yield (%)

$$= \frac{(\text{weight of upper layer} \times \% \text{methyl esters content})}{\text{weight of oil used}}$$

3.5 Catalyst preparation

3.5.1. Acid catalyst: supported heteropolyacid

The catalyst 12-tungstophosphoric acid (HPW) supported onto silica was synthesized as described in [34]. A series of catalysts containing 15-80% HPW, $\text{H}_3\text{PW}_{12}\text{O}_{40} \cdot 6\text{H}_2\text{O}$, was synthesized by impregnating 1 g of SiO_2 with an aqueous solution of $\text{H}_3\text{PW}_{12}\text{O}_{40} \cdot 6\text{H}_2\text{O}$ (0.15-0.80 g/15-80 mL of conductivity water) with stirring

for 35 h and dried at 100°C for 10 h. The materials were calcined at 300°C for 1 h. The obtained materials were designed as HPW/SiO₂

3.5.2 Base catalyst

3.5.2.1) Preparation of MgAl hydrotalcites

A. Alkali - free co-precipitation method

The MgAl hydrotalcite precursors at Mg/Al molar ratio 3 and 4 were prepared by co-precipitation method. An aqueous solution (90 mL) of 0.054 mol or 0.072 mol of Mg(NO₃)₂·6H₂O (for Mg/Al molar ratio 3 and 4, respectively) and 0.018 mol of Al(NO₃)₃·9H₂O were added slowly to a second solution (120 mL) of 0.1125 mol of (NH₄)₂CO₃ under vigorous mechanical stirring. The pH of the mixture was adjusted at 8 and 11 by dropwise addition of NH₄OH. The resulting mixture was heated to 65°C while stirred vigorously for 3 h, after which the product was left for 18 h. Then it was filtered and washed with distilled water until the filtrate was neutral. The precipitate was dried in an oven at 100°C for 18 h.

B. Alkali co-precipitation method

The alkali hydrotalcites were prepared similarly to alkali-free co-precipitation method, except that (NH₄)₂CO₃ and NH₄OH were replaced with Na₂CO₃ and NaOH, respectively.

3.5.2.2) Metal loaded catalysts

The hydrotalcites were calcined at 450°C for 35h to obtain mixed oxide (MgAlO). Loading metal onto mixed oxide was loaded using impregnation method. The metal salt dissolved in a minimum volume of distilled water was added into the mixed oxide powder and the mixture was stirred at room temperature for 1 h. Then, it was air dried at

100°C for 12 h and calcined at 600°C for 2 h. The obtained were designed as M MgAlO (metal loaded mixed oxide)

3.5.2.3) Preparation of calcined and rehydrated MgAlLa hydrotalcites

For hydrotalcite containing La having Mg^{2+}/M^{3+} molar ratio 4 ($M^{3+} = Al + La$), the solution A contained 0.10 mol $Mg(NO_3)_2 \cdot 6H_2O$ and 0.023 $Al(NO_3)_3 \cdot 9H_2O$ and 0.002 mol $La(NO_3)_3 \cdot 6H_2O$ for La low catalyst or 0.020 mol $Al(NO_3)_3 \cdot 9H_2O$ and 0.005 mol $La(NO_3)_3 \cdot 6H_2O$ for La high catalyst dissolved in distilled water (150 mL). The solution A was added to the solution B which contained (120 mL) 0.1125 mol $(NH_4)_2CO_3$ and NH_4OH was added to adjust pH to 11 under vigorous mechanical stirring. The resulting gel was matured by heating it at 65°C for 18 h. Then, it was filtered and washed with distilled water until the pH of the wash water was neutral.

The obtained Mg(Al)La hydrotalcite was calcined at 460°C for 18 h to yield Mg(Al)LaO. The Mg(Al)LaO was rehydrated by placing it in a desiccator saturated with water for 48 h.

3.5.2.4) Test of metal leaching from catalyst

Catalyst was stirred in methanol at 60°C for 3 h, and filtered. The filtrate was then reacted with glyceryl tributyrate. The product was analyzed by gas chromatography (GC) using decane as an internal standard.

3.5.2.5) Reusability of catalyst

At the end of transesterification of glyceryl tributyrate reaction the catalyst was separated by filtration and washed with methanol. Then, it was calcined at 460°C 5 h. The recovered catalyst was used for transesterification of glyceryl tributyrate to observe its remaining activity. The product was analyzed by gas chromatography (GC) using decane as an internal standard.

3.6 Treatment of crude rice bran oil

3.6.1 Water degumming of crude rice bran

Crude rice bran oil (500 g) was vigorously stirred for 30 min then 50% v/v cold water was added with stirring. The mixture was centrifuged at 4000 rpm for 15 min. The oil was separated and heated about 30 min and added 25% v/v 75% H₃PO₄ without stirring. After that, 50% v/v hot water was added with stirring for 2 h. The mixture was centrifuged at 4000 rpm for 15 min. Rotary evaporation was used to remove the residual water from degummed oil.

3.6.2 Free fatty acid measurement

Free fatty acid in crude rice bran oil was measured by titration method according to the procedure as describe in [35]. Crude rice bran oil (2.0 g) was mixed with 50 mL neutralized 2-propanol by adding 2 mL phenolphthalein solution and 0.1 M KOH to produce faint permanent pink. This mixture was titrated with 0.25M KOH with vigorous shaking until permanent faint pink appeared and persisted more than 1 min. Free fatty acids (expressed as oleic acid) were calculated from volume of 0.25 NaOH used in titration.

$$\% \text{ Free fatty acid} = \frac{\text{volume of base solution} \times \text{base concentration} \times 25.6}{\text{weight of oil}}$$

3.7 Catalytic activity

3.7.1 Transesterification of glyceryl tributyrate

In a 100 mL round bottom flask equipped with a stirrer and a reflux condenser, 12.5 mL (0.30 mol) of methanol and 0.05 g (1.5% w/w glyceryl tributyrate) catalyst were added. Then 3 mL (0.01 mol) of glyceryl tributyrate was added. The temperature was set

to 60°C. After 3 h, the sample was analyzed by gas chromatography (GC) using decane as an internal standard.

3.7.2 Esterification of free fatty acid in crude rice bran oil

Crude rice bran oil was mixed with methanol (10:1 molar ratio of methanol to oil) and varying amount of catalysts for a specified period, and then the catalyst was removed by centrifuging and the excess of methanol was recovered under vacuum at the 60°C with a rotational evaporator. The mixture was left to settle to separate into two layers. The methanol-water fraction at the top layer was removed. The FFA content of the product separated at the bottom was determined by method as section 3.6.2.

The conversion of FFA in the crude rice bran oil to biodiesel was calculated from following equation:

$$\text{Conversion \%} = (\text{FFA}_0 - \text{FFA}_1 / \text{FFA}_0) \times 100\%$$

FFA₀ is the initial free fatty acid in crude rice bran oil

FFA₁ is the remaining free fatty acid in crude rice bran oil

3.7.3 Tranesterification of treated rice bran oil

Transesterification of rice bran oil was carried out in either a 100 ml round bottom flask equipped with magnetic stirrer and reflux condenser or a Parr reactor. After the reaction, the catalyst was filtered by filter paper. The mixture was put into a separating funnel. The upper layer was methyl ester and the lower layer was glycerol [2]. The methyl ester was separated. The excess methanol was evaporated using rotary evaporator. The methyl ester was washed with saturated NaCl solution and distilled water to separate glycerol and soap. Sodium sulfate anhydrous was added to remove water in the methyl ester product.

The reaction was studied by varying various parameters as follows:

- Molar ratio of methanol/oil
- Catalyst amount



สถาบันวิทยบริการ
จุฬาลงกรณ์มหาวิทยาลัย

CHAPTER IV

RESULTS AND DISCUSSION

4.1 Preparation of catalysts

Base and acid catalysts were synthesized to catalysis in transesterification and esterification of crude rice bran oil to obtain fatty acid methyl ester (biodiesel).

Base catalysts were synthesized for catalysis in transesterification of glyceryl tributyrates as model compound of vegetable oil and crude rice bran oil to obtain fatty acid methyl ester. MgAl hydrotalcites precursors were synthesized by two different methods: alkali-free co-precipitation and alkali co-precipitation methods. The first method utilised $(\text{NH}_4)_2\text{CO}_3$ while the latter used NH_4OH as the precipitation agent. Furthermore, molar ratio of Mg/Al in hydrotalcites and pH values of co-precipitation on the formation of hydrotalcites were also varied to study the reaction parameters affecting catalytic activity of the synthesized catalyst. In order to increase the catalytic activity of hydrotalcites, calcinations of hydrotalcites to obtain mixed oxide (MgAlO) and loading metal onto MgAlO was performed to obtain metal loaded mixed oxide (M-MgAlO). The other one of base catalyst was Mg(Al)La hydrotalcites precursors which were also synthesized by co-precipitation method. Mg(Al)La hydrotalcites were calcined at high temperature to obtain Mg(Al)LaO and then Mg(Al)LaO was rehydrated to restore the structure to hydrotalcites.

Acid catalysts were synthesized for catalysis in esterification of free fatty acid in crude rice bran oil to reduce free fatty acid content in crude rice bran oil. Supported heteropolyacid was synthesized by impregnation 15-80 wt% of $\text{H}_3\text{PW}_{12}\text{O}_{40}$ (HPW) onto silica. The chart of synthesized catalysts is presented in Figure 4.1.

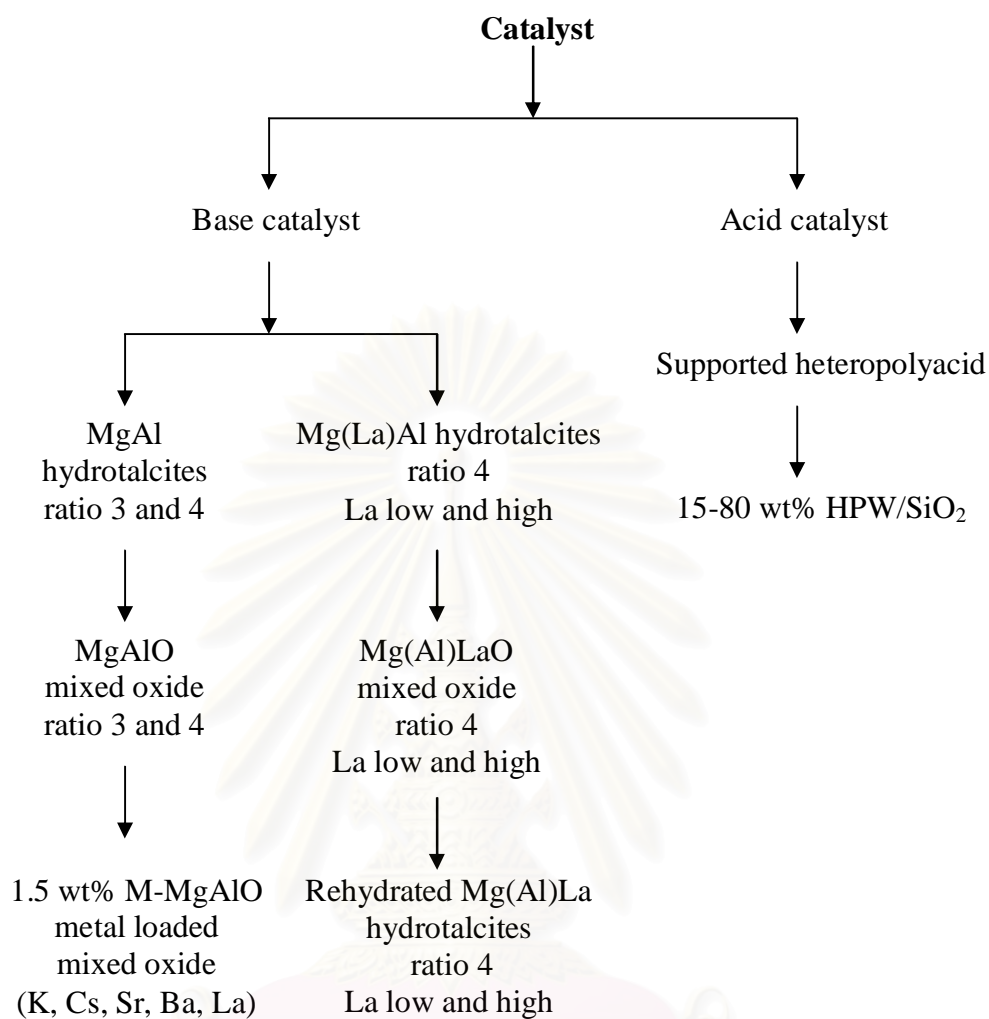


Figure 4.1 The chart of synthesized catalysts.

4.2 Base Catalysts

Solid base MgAl hydrotalcites and Mg(Al)La hydrotalcites precursors were synthesized by co-precipitation method. To obtain mixed oxide, hydrotalcites precursors were calcined at high temperature.

4.2.1 Characterization of catalysts

4.2.1.1) MgAl hydrotalcites and MgAlO mixed oxide catalysts

MgAl hydrotalcites were synthesized by varying co-precipitation method, Mg/Al molar ratio and pH values of formation of hydrotalcites. The synthesized catalysts were characterized by ICP-AES, XRD, SEM, BET, FT-IR and basicity was measured by titration method.

4.2.1.1.1) Metal content in MgAl hydrotalcites

The successful incorporation of Mg and Al within the $[\text{Mg}_{(1-x)}\text{Al}_x(\text{OH})_2]^{x+}(\text{CO}_3)_{x/n}^{2-}$ hydrotalcites was verified by inductively coupled plasma emission spectrometry. The nominal and measured Mg/Al molar ratio is presented in Table 4.1.

Table 4.1 The nominal and measured Mg/Al molar ratio

Nominal	Measured
3	1.72
4	2.54

The data revealed the deviation between nominal and measured Mg/Al molar ratio. This deviation is due to the pH used in the preparation. The low pH value disfavored the incorporation of Mg^{2+} in hydrotalcites due to the relatively high solubility of $\text{Mg}(\text{OH})_2$ ($K_{\text{sp}} = 7.1 \times 10^{-12}$) in comparison with that of $\text{Al}(\text{OH})_3$ ($K_{\text{sp}} = 1.3 \times 10^{-33}$) [36].

4.2.1.1.2) Structure and the composition of the materials

The synthesized hydrotalcites by alkali-free and alkali co-precipitation methods are characterized the structure by XRD technique. The XRD patterns of MgAl hydrotalcite (Mg/Al molar ratio 3) are shown in Figure 4.2.

Alkali free method

Alkali method

Figure 4.2 XRD Patterns of MgAl hydrotalcites (Mg/Al molar ratio 3).

The XRD pattern (Figure 4.2) of the MgAl hydrotalcite presents the typical pattern of a pure layered double hydroxide structure [10]. The diffraction peaks were observed at $2\theta = 11.6, 23.2, 34.8, 39.2, 60.8$ and 62.2 which corresponded to the hydrotalcites in hexagonal crystal system, the result was in good agreement with that reported in the literature [5]. Plane spacings of synthesized MgAl hydrotalcites are presented in Table 4.2.

Table 4.2 Plane spacings of synthesized MgAl hydrotalcites (Mg/Al molar ratio 3)

MgAl hydrotalcites		
hkl	$2\theta(^{\circ})$	$d(\text{\AA})$
003	11.6	7.62
006	23.2	3.82
012	34.8	2.58
015	39.2	2.30
110	60.8	1.52
113	62.2	1.50

The unit cell dimensions of MgAl hydrotalcites in hexagonal crystal system prepared with both alkali and alkali free methods are calculated as follows [10]:

$$a = 2xd_{110}$$

$$c = 3 / 2x(d_{003} + 2d_{006})$$

The lattice parameter c was related to the interlayer distance. It mainly depended on the hydrated anion size and on the electrostatic forces between the layers and interlayer anions that were affected by the degree of trivalent cations substitution of Mg^{2+} in the brucite sheet. The lattice parameter a was related to the unit cell dimension which increase with Mg^{2+} content. This expansion of the lattice parameter was again consistent with the direct substitution of Al^{3+} by Mg^{2+} within the 'brucite like' layers and confirmed that a solid solution was formed, rather than discrete phase [10]. The unit cell dimensions of hexagonal hydrotalcites are shown in Table 4.3 They are in good agreement with that reported [21].

Table 4.3 Unit cell dimensions of MgAl hydrotalcites (Mg/Al molar ratio 3)

Method	Crystal system	Unit cell dimensions	
		$a(\text{\AA})$	$c(\text{\AA})$
alkali	hexagonal	3.06	22.95
alkali free	hexagonal	3.06	22.88

In addition, effect of pH on the property of MgAl hydrotalcite catalyst was investigated. The XRD patterns of the MgAl hydrotalcites precursors (molar ratio 3) prepared at pH 8 vs 11 are shown in Figure 4.2. The diffraction peaks at pH 11 were sharper than those at pH 8, indicating the increased particle size or improved crystallinity. In addition, at pH 8 there appeared minor reflection at $2\theta = 20.5$ which was $MgAl_2(OH)_8$ [10].

MgAl Hydrotalcite pH 11

MgAl Hydrotalcite pH 8

*

Figure 4.3 XRD Patterns of MgAl hydrotalcites molar ratio = 3 at pH 8 and 11.
Asterisk (*) indicates peaks corresponding to $\text{MgAl}_2(\text{OH})_8$ phase

In order to determine the influence of Mg/Al ratio of hydrotalcites on their catalytic activity, hydrotalcites with different Mg/Al molar ratio (Mg/Al = 3 and 4) were prepared at pH 11. The layered structure was confirmed by their characteristic XRD patterns as in Figure 4.4.



Figure 4.4 XRD Patterns of MgAl hydrotalcites, Mg/Al molar ratio = 3 and 4.
Asterisk (*) denotes corresponding to $\text{Mg}_5(\text{CO}_3)_4(\text{OH})_2 \cdot 4\text{H}_2\text{O}$ phase

For the sample prepared with Mg/Al molar ratio = 3, a shift to higher 2θ was observed in Table 4.4

Table 4.4 Plane spacings of MgAl hydrotalcites molar ratio 3 and 4

MgAl hydrotalcites molar ratio 3		MgAl hydrotalcites molar ratio 4	
hkl	2 θ (°)	hkl	2 θ (°)
003	11.6	003	11.3
006	23.2	006	23.0
012	34.8	012	34.7
015	39.2	015	38.9
110	60.8	110	60.6
113	62.2	113	61.8

The plane spacing reflects decreased interlayer distance and unit cell parameters [37]. The unit cell dimensions of hexagonal hydrotalcites are shown in Table 4.5. This is in good agreement with previous reported [10]. Furthermore, minor reflections at 15.2° and 31.9° for sample with Mg/Al ratio 4 were attributed to Mg₅(CO₃)₄(OH)₂·4H₂O phase [10].

Table 4.5 Unit cell dimensions of MgAl hydrotalcites molar ratio 3 and 4

Mg/Al molar ratio	Crystal system	Unit cell dimensions	
		a(Å)	c(Å)
3	hexagonal	3.06	22.88
4	hexagonal	3.06	23.11

In order to obtain MgAlO (mixed oxide), MgAl hydrotalcites were calcined at 450°C for 35 h, it was found that the diffraction peaks were shifted, indicating the structure change of material [24]. The diffraction peaks were observed at $2q = 35.7$, 43.2 and 62.6 which corresponded to cubic MgAlO phase. The XRD patterns of MgAlO (Mg/Al molar ratio 4) compared with MgAl hydrotalcite are presented in Figure 4.5 and plane spacings of MgAlO are presented in Table 4.6.

MgAlO

MgAl hydrotalcite

Figure 4.5 XRD Patterns of MgAlO (Mg/Al molar ratio 4) compared with MgAl hydrotalcite.

Table 4.6 Plane spacings of MgAlO (Mg/Al molar ratio 4)

MgAlO		
hkl	2 θ (°)	d(Å)
110	35.7	2.51
200	43.2	2.09
220	62.6	1.48

Furthermore, the a value for cubic MgAlO (Mg/Al molar ratio 4) compared with other work are presented in Table 4.7. It can be seen that the a values of synthesized MgAlO was close and in good agreement with that reported [24, 38]

Table 4.7 Unit cell dimensions of MgAlO molar ratio 4

Method	Crystal system	Unit cell dimensions	Ref
		a (Å)	
alkali	Cubic	4.25	In this work
alkali	Cubic	4.26	[24]
alkali free	Cubic	4.24	In this work
alkali free	Cubic	4.24	[38]

In this work, in order to increase the basicity of catalyst, some alkali and alkali earth metals were prepared using impregnation method with potassium acetate, cesium nitrate, strontium nitrate, barium nitrate and lanthanum nitrate as a precursor salt. XRD patterns of MgAlO loaded with different metals are shown in Figure 4.6.

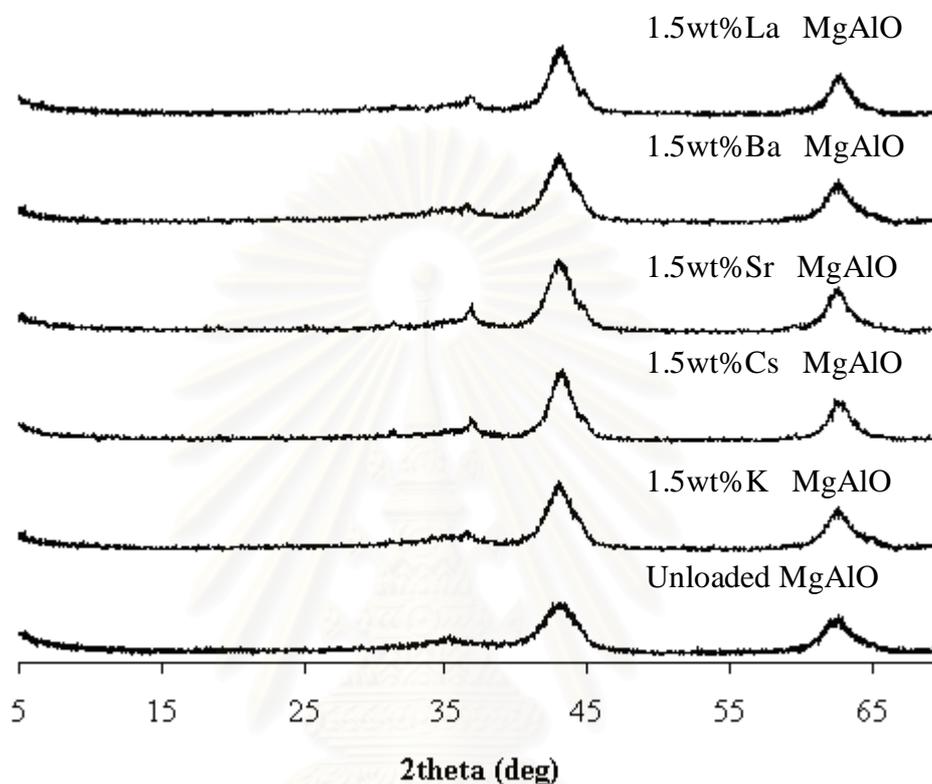


Figure 4.6 XRD Patterns of MgAlO loaded with different metal.

The introduction of metal into the MgAlO did not cause any change in the structure of the support. These XRD patterns were also similar to that reported [33] which indicating the high dispersion of metal species on the surface [39].

4.2.1.1.3) The morphology of catalysts

To determine the morphology of the metal loaded mixed oxide, the 1.5wt%K MgAlO catalyst was selected to study by scanning electron microscopy (SEM) and compared to the MgAl hydrotalcite. The SEM images of MgAl hydrotalcite and 1.5wt%K MgAlO are shown in Figure 4.7.

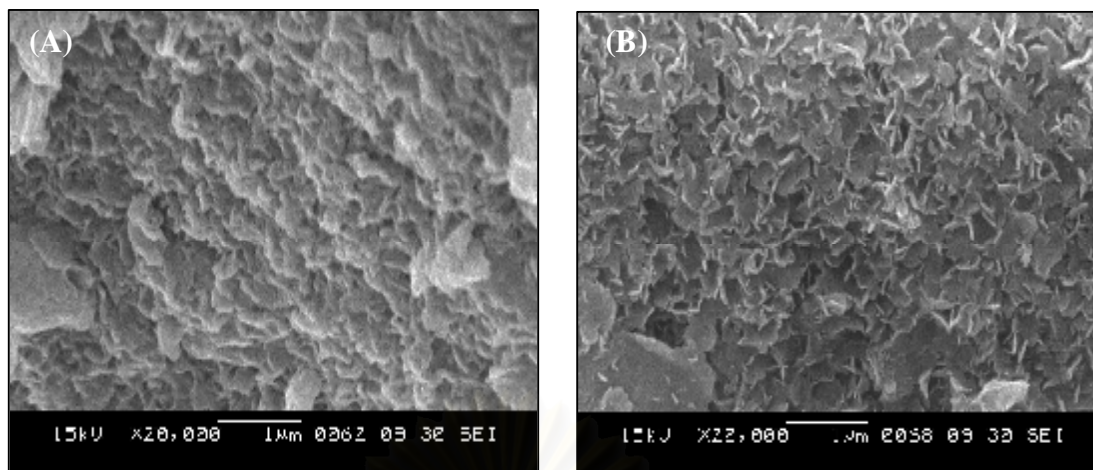


Figure 4.7 SEM images (x20,000 magnification) of
(A) MgAl hydrotalcite (B) 1.5% K loaded MgAlO

It can be observed clearly from SEM image of MgAl hydrotalcite in Figure 4.7A that MgAl hydrotalcite formed well-developed, thin flat crystal indicating the layer structure and still remained in the metal loaded mixed oxide (Figure 4.7B). This is in good agreement with the results reported previously [40], which show that upon heating, water and CO₂ are released by a cratering mechanism rather than by exfoliation and that the crystal morphology is preserved.

4.2.1.1.4) Surface area and porosity of catalyst

Nitrogen sorption measurement is another method used for the determination of surface area and porosity of catalysts. The specific surface area of catalyst was calculated using BET method. Their total pore volume was obtained from the desorption volume at $P/P_0 = 0.98$ and mean pore diameter was calculated from $4V_p/S$.

BET specific surface areas and porosity of MgAl hydrotalcites molar ratio 4 was 102 m²/g with total pore volume 0.86 cm³/g and mean pore diameter 33.74 nm. In order to obtain MgAlO, MgAl hydrotalcites was calcined at 450°C for 35h. The obtained N₂ sorption isotherm of MgAlO is displayed in Figure 4.8.

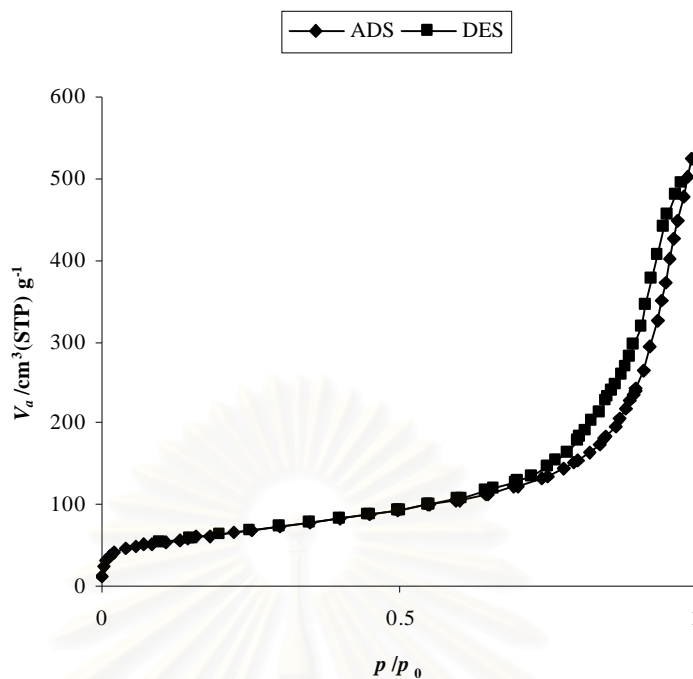


Figure 4.8 N₂ adsorption-desorption isotherm of MgAlO.

As seen from Figure 4.8, MgAlO showed irreversible type IV adsorption isotherm with a H1 hysteresis loop as defined in the IUPAC [41]. A linear increase of adsorbed volume at low temperature followed by a steep increase in nitrogen uptake at a relative low pressure was observed, which was characteristic for solid consisting of cylindrical pores of uniform size and shape as dominant. This result was in accordance with the previous work reported by Kustrowski *et al.* [42]. In addition, the textural properties obtained from N₂ sorption measurement are also summarized in Table 4.8.

Table 4.8 The textural properties of MgAlO catalysts

Method	Calcination time (h)	BET surface area, S (m ² /g)	Total pore volume, V _p (cm ³ /g)	Mean pore diameter, MPD (nm)
alkali	5	169	1.06	25
alkali	35	240	1.09	19
alkali free	35	237	0.98	17

S, BET surface area obtained from N₂ sorption; V_p, total pore volume obtained from single-point volume at $P/P_0 = 0.98$; MPD, mean pore diameter calculated from $4V_p/S$

The calcination of hydrotalcite resulted in increased surface area. It has been reported [40] that the decomposition of hydrotalcite preserved the overall particle shape. Moreover, longer calcination time was need for high surface area. The MgAlO samples prepared by both methods gave comparable surface area.

Metal loaded mixed oxide was also measured BET specific surface areas and porosity. The obtained N₂ sorption isotherm of 1.5wt%K MgAlO was selected to be representative of metal loaded mixed oxide is displayed in Figure 4.9.

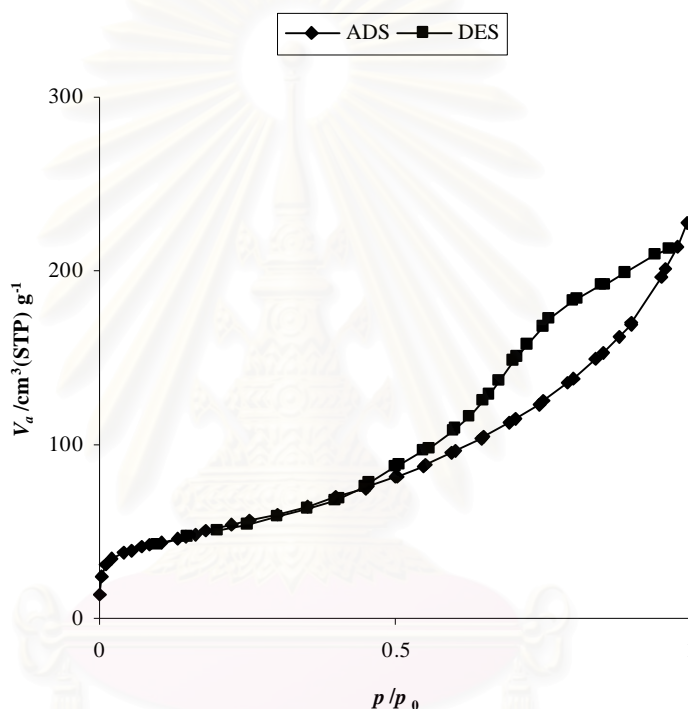


Figure 4.9 N₂ adsorption-desorption isotherm of metal loaded mixed oxide.

Metal loaded mixed oxide still showed a mesoporous solid due to an adsorption/desorption isotherm was still type IV adsorption isotherm with a H4 hysteresis loop as defined in the IUPAC [41]. In addition, the textural properties obtained from N₂ sorption measurement are also summarized in Table 4.9.

Table 4.9 The textural properties of metal loaded mixed oxide catalysts

Mg/Al molar ratio	Metal Load (1.5 wt%)	BET surface Area, S (m²/g)	Total pore volume, V_p (cm³/g)	Mean pore diameter, MPD (nm)
3	None	237	0.98	17
	K	137	0.30	9
	Cs	147	0.30	8
	Sr	163	0.30	7
	La	158	0.32	8
4	None	232	0.79	14
	K	140	0.24	7
	Cs	156	0.28	7
	Sr	172	0.26	6
	La	159	0.29	7

S, BET surface area obtained from N₂ sorption; V_p, total pore volume obtained from single-point volume at $P/P_0 = 0.98$; MPD, mean pore diameter calculated from $4V_p/S$

When loading metal onto the mixed metal oxide, the surface area and pore volumes were decreased, resulting from the incorporation of occluded metal oxide species. This result was in accordance with the previous work reported [43].

4.2.1.1.5) Functional group of catalysts

Functional group of catalysts was characterized by Fourier-transform infrared spectra (FT-IR). The spectra of MgAl hydrotalcites prepared with two methods at different conditions gave similarly spectra. In order to compare the spectra of MgAl hydrotalcites, mixed oxide and metal loaded mixed oxide, 1.5wt% MgAlO was selected to be representative of metal loaded mixed oxide. The representative FT-IR spectra are shown in Figure 4.10.

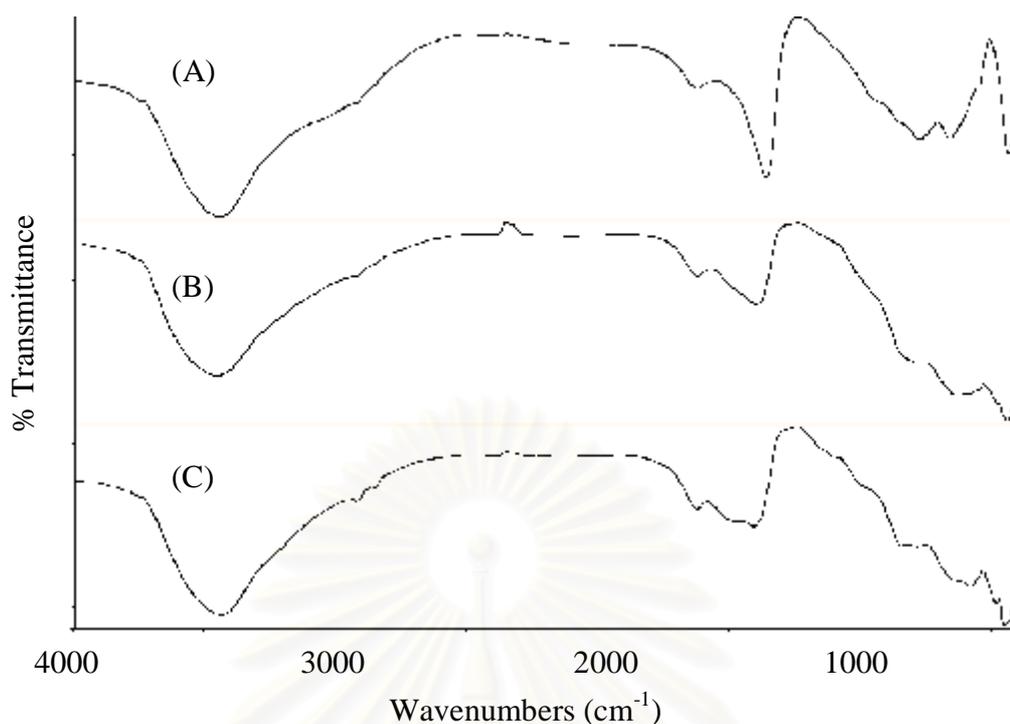


Figure 4.10 FT-IR spectra of
 (A) MgAl hydrotalcite (B) MgAlO (C) 1.5wt% MgAlO.

In Figure 4.10(A) the absorption band around 3400 cm^{-1} was attributed to O-H vibration mode of hydroxyl group and water molecules. Another absorption band corresponding to water deformation was observed at 1626 cm^{-1} . The bands below 850 cm^{-1} were due to the vibrations of $M\text{-O}$ ($M = \text{Mg}^{2+}, \text{Al}^{3+}$). The bands at 1370 and 670 cm^{-1} correspond to the vibration of the interlayer anion (CO_3^{2-}) and $M\text{-O}$ [37].

After calcination of hydrotalcite (MgAlO) (Figure 4.10(B)), the band at 1370 cm^{-1} attributed to carbonates was broad with lower intensity than MgAl hydrotalcites. However, this band was still present, this might due to the readsorption of gaseous CO_2 (coming for the ambient atmosphere) on the basic site of the MgAlO or no totally decomposed carbonates at this temperature [24].

Thus, FT-IR spectrum confirmed that calcination at 450°C for 35h indicated to decomposition of CO_2 in MgAl hydrotalcites to form MgAlO. However, the FT-IR spectrum of 1.5wt% MgAlO (Figure 4.10(C)) was similar to that of MgAlO.

4.2.1.1.6) Soluble basicity of the catalysts

The soluble basicity of various mixed oxides were determined by titration with benzoic acid. It was reported the MgAlO contains surface basic sites of low (OH group), medium (Mg-O pairs) and strong (O^{2-}) basicity. The soluble basicity of the catalysts are shown in Table 4.10

Table 4.10 Soluble basicity of catalysts

metal loaded	Soluble basicity (mmol/g)	
	Mg/Al molar ratio	
	3	4
1.5 wt%		
Unloaded	0.16*	ND
Unloaded	0.01	0.02
K	0.20	0.23
Cs	0.03	0.04
Sr	0.03	0.03
Ba	0.05	0.06
La	0.02	0.02

* alkali method

ND = not determined

From Table 4.9, it could be seen that the soluble basicity of mixed oxide prepared with alkali method was much higher than that with the alkali-free method. The mixed oxide with Mg/Al ratio of 4 also showed higher soluble basicity than the one of 3. When metal was loaded, the soluble basicity of the metal loaded mixed oxide catalysts also increased. This is in agreement with previous report [44], in which metal ions were introduced to replace the protons [33]. Experimental results in this work showed that all the samples gave low soluble basicity except for K loaded metal onto MgAlO.

4.2.2.1 Mg(Al)La hydrotalcite and Mg(Al)LaO catalysts

4.2.2.1.1) Structure and the composition materials

Mg(Al)La hydrotalcite precursors has also been synthesized and calcined at 460°C for 16h to obtain Mg(Al)LaO. XRD patterns of Mg(Al)La hydrotalcite showed the diffraction peaks at $2q = 11.6, 23.1, 34.2, 39.3, 60.6$ and 62.0 with other phases: La_2CO_5 (JCPDS 23-0320) and $\text{La}_2(\text{CO}_3)_2(\text{OH})_2$ (JCPDS 70-1774) phases [22]. The strong anionic character of La (electronegativity 1.1) favored the formation of carbonate species in the very early stage of the co-precipitation. The XRD patterns of Mg(Al)La hydrotalcite is shown in Figure 4.11.

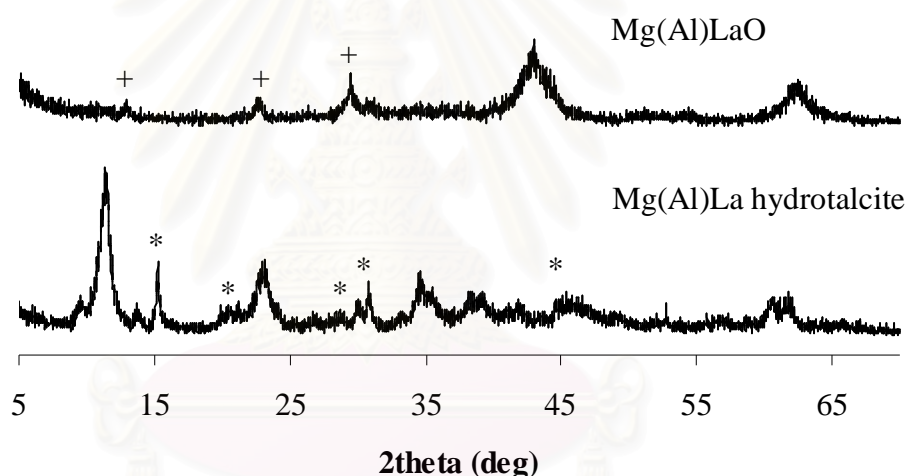


Figure 4.11 XRD patterns of Mg(Al)La hydrotalcite and the Mg(Al)LaO. Asterisk (*) indicates peaks corresponding to a La_2CO_5 and $\text{La}_2(\text{CO}_3)_2(\text{OH})_2$ phases.

Plus (+) denotes peaks corresponding to a $\text{La}_2\text{O}_2\text{CO}_3$ [21].

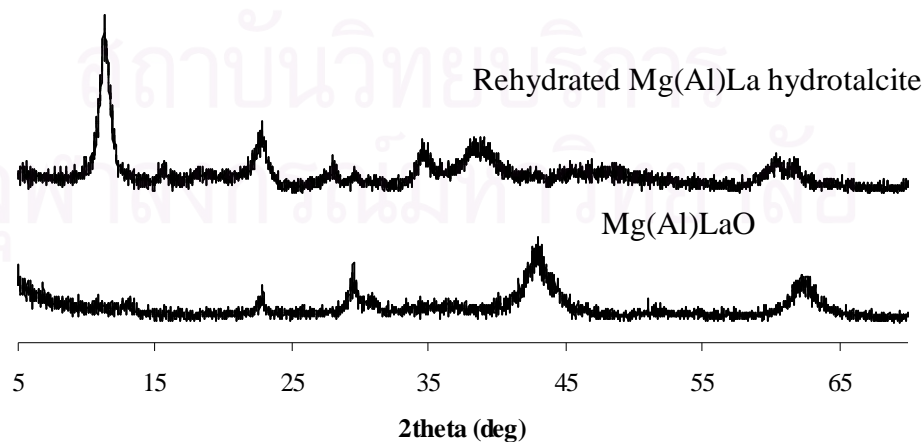
In order to obtain Mg(Al)LaO, Mg(Al)La hydrotalcites were calcined at 460°C for 18 h leading to Mg(Al)LaO (as shown in Figure 4.11). Furthermore, $\text{La}_2\text{O}_2\text{CO}_3$ phase which was formed by readsorption of gaseous CO_2 , coming from the hydrotalcites decomposition or by air can be observed. The unit cell dimensions of Mg(Al)La hydrotalcite are calculated as same as MgAl hydrotalcite (as section 4.2.1.2.2). The lattice parameters Mg(Al)La hydrotalcite and Mg(Al)LaO are reported in Table 4.11.

Table 4.11 Lattice parameters of Mg(Al)La hydrotalcite and Mg(Al)LaO

Catalyst	Crystal system	Lattice parameters	
		$a(\text{\AA})$	$C(\text{\AA})$
MgAl hydrotalcites	Hexagonal	3.06	22.88
Mg(Al)La hydrotalcite	Hexagonal	3.05	23.33
MgAlO	Cubic	4.24	-
Mg(Al)LaO	Cubic	4.24	-

The lattice parameter data indicated that there was no modification of lattice parameter a but the lattice parameter c value increased as a consequence of large ionic radius of La, the radius of Al^{3+} and La^{3+} were 0.535 Å and 1.032 Å, respectively [21].

When performing rehydration on the Mg(Al)LaO, it was found that the original layered structure can be restored due to the diffraction peaks at $2q = 11.6, 23.1, 34.2, 39.3, 60.6$ and 62.0 can be observed. The rehydrated Mg(Al)La hydrotalcites contained OH^- ions in the interlayer which act as Brønsted basic site with a stronger basicity than CO_3^{2-} ions located into the hydrotalcites structure [45]. Furthermore, La_2CO_5 and $\text{La}_2(\text{CO}_3)_2(\text{OH})_2$ phase can not be observed in XRD pattern of rehydrated Mg(Al)La hydrotalcite. The XRD patterns of Mg(Al)La and rehydrated Mg(Al)La hydrotalcites are presented in Figure 4.12.

**Figure 4.12** XRD patterns of Mg(Al)LaO and rehydrated Mg(Al)La hydrotalcite.

4.2.2.1.2) Metal content in Mg(Al)LaO

In order to study the effect of lanthanum amount, the catalyst with different amount of lanthanum was synthesized. The metal contents of Mg(Al)LaO catalysts analyzed by ICP-AES are presented in Table 4.12.

Table 4.12 The metal content of Mg(Al)LaO catalyst

Catalyst	Amount of metal (mmol)			Ratio of M(II)/M(III)
	Mg	Al	La	
Mg(Al)LaO (La low)	42.37	14.46	2.74	2.46
Mg(Al)LaO (La high)	31.67	8.15	5.83	2.27

The data suggested that the effect of the addition of La at the synthesis was a decreasing of the M(II)/M(III) ($Mg^{2+}/(Al^{3+} + La^{3+})$) molar ratio of catalyst in comparison with Mg/Al ratio of the corresponding free earth oxide syntheses. This result was in agreement with the previous reported [44].

4.2.2.1.3) The morphology of catalysts

The morphology of Mg(Al)LaO and rehydrated Mg(Al)La hydrotalcites formation was taken as scanning electron micrographs. Their SEM images are presented in Figure 4.13.

สถาบันวิทยบริการ
จุฬาลงกรณ์มหาวิทยาลัย

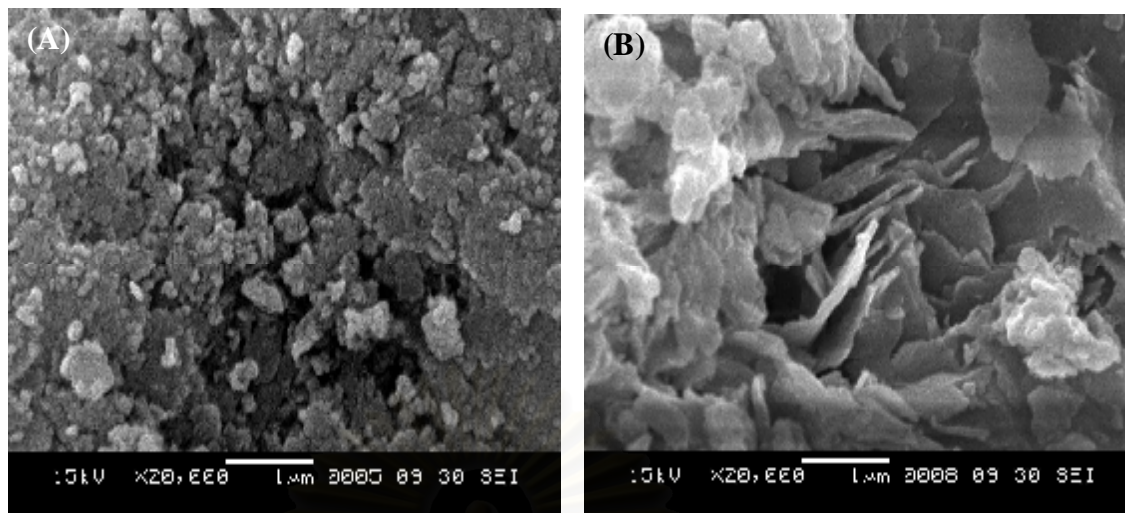


Figure 4.13 SEM images ($\times 20,000$) of

(A) Mg(Al)LaO

(B) Rehydrated Mg(Al)La hydroxalcite

The SEM photograph of Mg(Al)LaO (Fig. 4.13A) still showed thin flat crystal. However, after rehydration it was possible to observe the formation of rigid and flat plates (Fig. 4.13B) resembled to SEM photograph of MgAl hydroxalcite indicating the layer structure.

4.2.2.1.4) Surface area and porosity of catalyst

The surface area and porosity of Mg(Al)LaO (La low) catalyst are determined by BET technique as same as metal loaded mixed oxide. In order to obtain Mg(Al)LaO, Mg(Al)La hydroxalcite was calcined at 460°C for 16h. The obtained N_2 sorption isotherms are displayed in Figure 4.14.

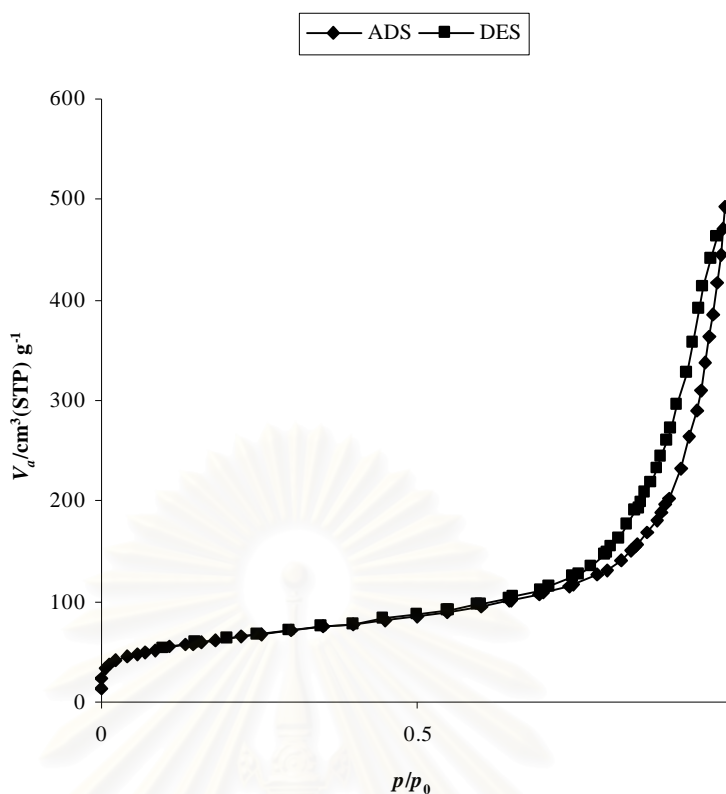


Figure 4.14 N₂ adsorption-desorption isotherm of Mg(Al)LaO.

Both of Mg(Al)LaO La low and La high presented the same N₂ adsorption-desorption are displayed in Figure 4.14 which were same as N₂ adsorption-desorption of MgAlO (as section 4.2.1.1.4) indicating mesoporous solid. This result was in accordance with the previous work [45]. In addition, the textural structure properties obtained from the N₂ sorption measurement are also summarized in Table 4.13.

Table 4.13 The textural properties of Mg(Al)LaO catalyst.

Catalyst	BET surface area, S (m ² /g)	Total pore volume, V _p (cm ³ /g)	Mean pore diameter, MPD (nm)
Mg(Al)LaO (La low)	225	0.75	13
Mg(Al)LaO (La high)	195	0.49	10

S, BET surface area obtained from N₂ sorption; V_p, total pore volume obtained from single-point volume at $P/P_0 = 0.98$; MPD, mean pore diameter calculated from $4V_p/S$

The rehydrated Mg(Al)La hydrotalcites were also measured BET specific surface areas and porosity. The obtained N₂ sorption isotherm of rehydrated Mg(Al)La hydrotalcites closely resembled N₂ sorption isotherm of Mg(Al)LaO. In addition, the textural structure properties obtained from the N₂ sorption measurement are also summarized in Table 4.14.

Table 4.14 The textural properties of rehydrated Mg(Al)La hydrotalcites catalyst.

Catalyst	BET surface area, S (m ² /g)	Total pore volume, V _p (cm ³ /g)	Mean pore diameter, MPD (nm)
Rehydrated Mg(Al)La HT (La low)	37	0.15	16
Rehydrated Mg(Al)La HT (La low)	18	0.16	35

S, BET surface area obtained from N₂ sorption; V_p, total pore volume obtained from single-point volume at $P/P_0 = 0.98$; MPD, mean pore diameter calculated from $4V_p/S$

The results suggested that when the rehydration was performed, BET surface area of Mg(Al)O was reduced because the interlayered space was occupied by OH⁻. This is in agreement with previous reported [46].

4.2.2.1.5) Soluble basicity of the catalysts

The soluble basicity of Mg(Al)LaO and rehydrated Mg(Al)La hydrotalcites (Mg(Al)La HT) catalysts which is determined by titration with benzoic acid is shown in Table 4.15.

Table 4.15 Soluble basicity of La containing catalysts

Catalyst	Soluble basicity (mmol/g)
MgAlO	0.02
Mg(Al)LaO (La low)	0.16
Mg(Al)LaO (La high)	0.34
Rehydrated Mg(Al)La HT (La low)	0.10
Rehydrated Mg(Al)La HT (La high)	0.25

Compared to the MgAlO catalyst, Mg(Al)LaO catalysts have higher soluble basicity and the soluble basicity were dependent on amount of La. The addition of La resulted in more basic catalyst because of the basic character of La_2O_3 , which is close to CaO [45].

The rehydrated Mg(Al)La hydrotalcite had soluble basicity lower than Mg(Al)LaO due to the fact that the rehydrated Mg(Al)La hydrotalcite restored the layer structure of hydrotalcites and introduced intercalated OH^- counter ions, leading to decrease of medium (Mg-O pairs) and strong (O^{2-}) basicities [47].

4.2.2 Transesterification of glyceryl tributyrate

4.2.2.1 Catalytic activity of MgAlO catalysts

For screening catalytic activity of catalysts, the catalytic transesterification of glyceryl tributyrate with methanol to form methyl butanoate was performed under the same condition as catalyst amount 1.5 wt% based on glyceryl tributyrate with molar ratio of methanol to glyceryl tributyrate = 30 at 60°C for 3 h. This reaction condition was similar to that used by *Cantrell et al.* [10]. The activity was reported as % conversion of glyceryl tributyrate.

Since leached active species could be responsible for the catalytic activity. Thus, test of metal leaching of active site species in dissolution was required. If the leached metals are inactive for transesterification, then the catalyst is truly heterogeneous.

However, if the leached metals are catalytically active, then the catalysis is not entirely heterogeneous. The glyceryl tributyrate conversion using MgAlO catalyst are reported in Table 4.16.

Table 4.16 Glyceryl tributyrate conversion using MgAlO catalyst

Entry	Mg/Al Molar ratio	Method of co-precipitation	pH	Glyceryl tributyrate conversion (%)	Glyceryl tributyrate conversion (%) from leachate
1	3	alkali	11	70	33
2	3	alkali free	8	35	8
3	3	alkali free	11	40	10
4	4	alkali free	11	47	10

Reaction Condition : catalyst 1.5 wt% based on glyceryl tributyrate, 1.5 ml glyceryl tributyrate, 6.25 mL methanol, molar ratio of methanol to glyceryl tributyrate = 30, temperature 60°C, time 3 h

The comparison between MgAlO prepared with alkali co-precipitation (entry 1) and alkali-free co-precipitation (entry 3) had shown that the catalyst prepared with the alkali method gave higher glyceryl tributyrate conversion (70%) than the catalyst prepared with the alkali free method (40%). But the MgAlO prepared by alkali co-precipitation showed higher glyceryl tributyrate conversion from leachate indicating higher metal leaching, than those of alkali-free co-precipitation method. This would cause a problem of soap formation when used in transesterification of oil [28].

The influence of pH at co-precipitation presented that MgAlO synthesized at pH 11 (entry 2) gave higher glyceryl tributyrate conversion than material prepared at pH 8 (entry 3). This was due to the fact that material synthesized at pH 11 consisted of pure MgAl hydrotalcite and higher crystallinity as revealed in XRD patterns (as section 4.2.1.1.2).

The influence of MgAl molar ratio of hydrotalcites (entry 3 and 4) presented that the catalytic activity was improved with the increase MgAl molar ratio. This is in good agreement with the results reported previously [24]

4.2.2.2) Catalytic activity of metal-loaded MgAlO catalysts

The effect of metal loading amount on the catalytic activity of catalysts was studied. A series of K loaded mixed oxide was selected to investigate the catalytic activity. For comparison, the transesterification glyceryl tributyrate was performed under the same reaction conditions as in section 4.4.4.1. The catalytic activities are presented in Figure 4.15.

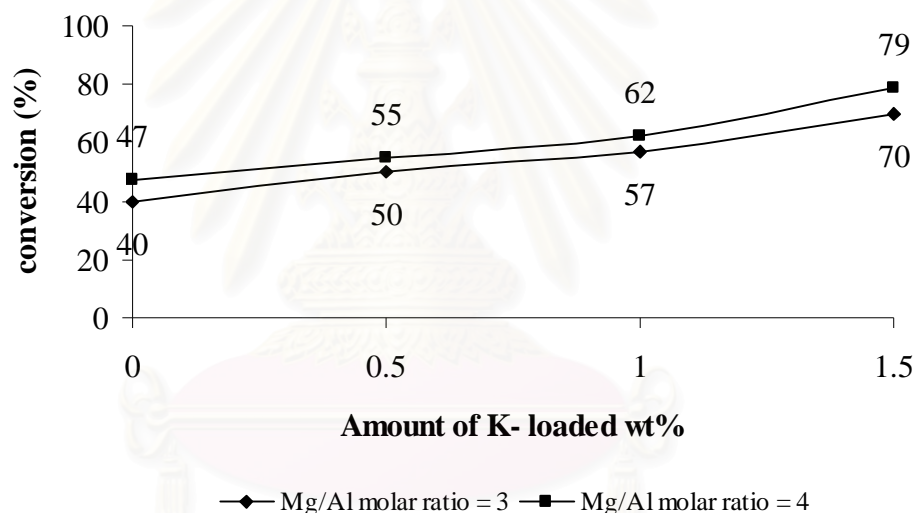


Figure 4.15 Catalytic activities of K- MgAlO with different amounts of metal and MgAl ratio.

The catalytic activities of various amounts of K loaded MgAlO catalysts were compared at the same condition. The catalytic activities of the K loaded mixed oxide gave higher than unloaded metal mixed oxide. The catalytic activity was increased with the amount of K loaded. This might be due to increasing number of basic sites [44].

Furthermore, the effect of different types of metal and Mg/Al molar ratio on the catalytic activity was studied at the same reaction condition as mentioned above. The catalytic activities are presented in Figure 4.16.

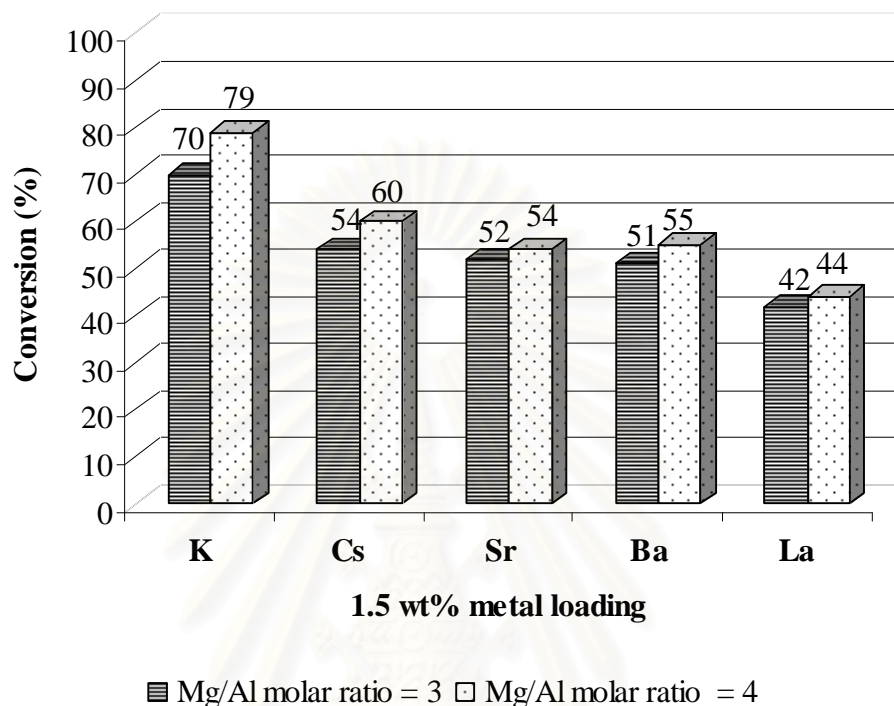


Figure 4.16 Catalytic activities of 1.5% wt metal loading with various metals and different Mg/Al molar ratios.

Among the catalysts tested, the MgAlO loaded with K catalysts were found to have higher catalytic activities than others, resulting in the conversion of 70-79%. Moreover, MgAlO ratio 4 also exhibited higher catalytic activity than MgAlO ratio 3. It can be concluded that 1.5wt% K MgAlO gave the highest glyceryl tributyrate conversion than those metal loaded mixed oxide. The higher catalyst activity could have resulted from the higher soluble basicity of the catalyst.

The catalytic activity order of metal is corresponding to the basic strength of the metal as follows: $K > Cs \sim Ba \sim Sr > La$.

The reuse of 1.5 wt% K MgAlO was investigated with the same reaction condition as before. It was shown that the reaction catalyzed by the recovered catalyst provided only 52% glyceryl tributyrate conversion, which was lower than the original

one (79%) catalyst. The recovered catalyst was characterized for soluble basicity. A decline of soluble basicity could be observed in the soluble basicity from 0.23 mmol/g to 0.09 mmol/g, leading to a drop of the catalytic activity of the spent catalyst. The reduced soluble basicity could be, probably, owing to the leaching of K species such as K_2O from the support catalysts [39].

4.2.2.3 Catalytic activity of Mg(Al)LaO catalysts and rehydrated Mg(Al)La hydrotalcite catalysts

For studying catalytic activity of Mg(Al)LaO catalysts, the catalytic transesterification of glyceryl tributyrate with methanol to form methyl butanoate was performed under the same condition as section 4.2.2.1. The catalytic activities are shown in Table 4.17.

Table 4.17 Transesterification of glyceryl tributyrate using Mg(Al)LaO and rehydrated Mg(Al)La hydrotalcites catalysts

Entry	Catalyst	Glyceryl tributyrate conversion (%)
1	MgAlO	47
2	Mg(Al)LaO (La low)	86
3	Mg(Al)LaO (La high)	100
4	Rehydrated Mg(Al)La HT (La low)	97
5	Rehydrated Mg(Al)La HT (La high)	100

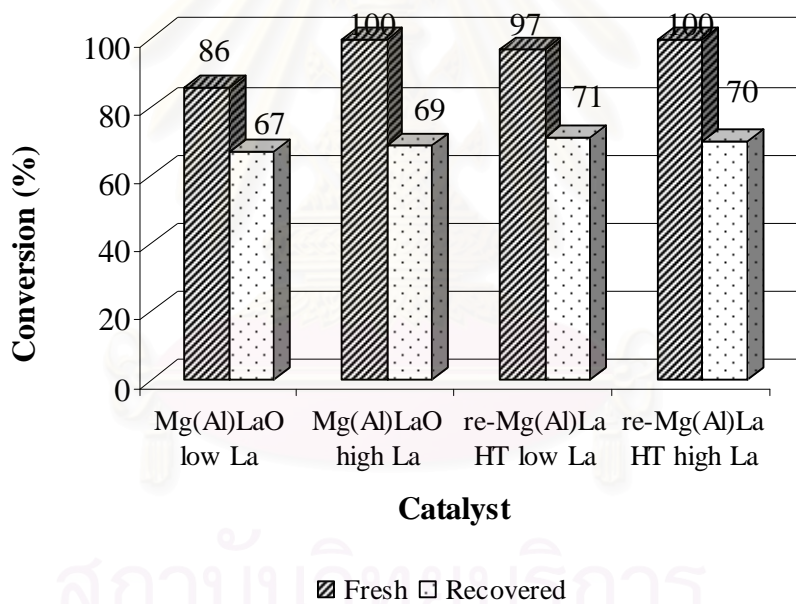
Reaction Condition : catalyst 1.5 wt% based on glyceryl tributyrate, 1.5 ml glyceryl tributyrate, 6.25 mL methanol, molar ratio of methanol to glyceryl tributyrate = 30, temperature 60°C, time 3 h

Compared Mg(Al)LaO with MgAlO catalyst, the result indicated that both of Mg(Al)LaO samples were considerably more active than MgAlO. Increasing the amount of La, the catalytic activity was also increased. The substitution of some Al by La resulted in more basic catalyst due to the high basic character of La_2O_3 .

The comparison of activity between Mg(Al)LaO and the rehydrated Mg(Al)La hydrotalcite catalyst, the rehydrated Mg(Al)La hydrotalcite samples were more active than the Mg(Al)LaO one. It might be due to the charged-balancing hydroxyl anions, i.e., the Brønsted base site, were more the active sites for the transesterification reaction than mixed oxide which exposed Lewis base sites [47].

4.2.2.4 Reusability of catalyst

In order to study the reusability of catalyst, catalysts were separated from reaction by filtration and were washed with methanol. The catalyst was calcined at 460°C for 5 h and reused for transesterification of glyceryl tributyrates under the same reaction condition as section 4.2.2.3. The results are presented in Figure 4.17.



Re-Mg(Al)La HT = rehydrated Mg(Al)La hydrotalcites

Figure 4.17 Catalytic activities of fresh catalyst and recovered catalyst.

It was shown that the reaction catalyzed by the recovered catalysts provided lower glyceryl tributyrates conversion than the fresh catalyst. It has been reported [48] that the decay of recovered catalyst may be due to deactivation of active site.

The soluble basicity of recovered catalysts was determined again and the results are also presented in Table 4.18.

Table 4.18 The soluble basicity of fresh and recovered catalysts

Entry	Catalyst	Soluble basicity (mmol/g) of catalyst	
		Fresh	Recovered
1	Mg(Al)LaO (La low)	0.16	0.13
2	Mg(Al)LaO (La high)	0.34	0.17
3	Rehydrated MgAlLa HT (La low)	0.10	0.09
4	Rehydrated MgAlLa HT (La high)	0.25	0.16

Reaction Condition : 0.025 g catalyst (1.5% wt based on glyceryl tributyrate), 1.5 ml glyceryl tributyrate, 6.25 mL methanol, molar ratio of methanol to glyceryl tributyrate = 30, temperature 60°C, time 3 h

The results showed that soluble basicity was decreased. Especially, the catalysts with high amount of La lead to much decreased of soluble basicity. This could be due to a leaching of the active phase to the alcoholic phase [48]. Therefore, the catalyst with high amount of La gave the high metal leaching to the reaction so the catalysis was not entirely heterogeneous.

It can be seen that the rehydrated Mg(Al)La hydrotalcite (La low) gave high catalytic activity of transesterification of glyceryl tributyrate and less of metal leaching than the other one. Thereby, the rehydrated Mg(Al)La hydrotalcite (La low) was selected as a catalyst for further study in the transesterification of the crude rice bran oil.

4.3 Acid Catalysts

Solid acid supported heteropolyacid was synthesized by impregnation method. The synthesized catalysts were characterized by XRD, BET, TPD, FT-IR.

4.3.1 Characterization of catalysts

4.3.1.1 Heteropolyacid supported onto Silica

As heteropolyacid (HPAs) is soluble in water indicating homogeneous catalyst which can not be reused and must be neutralized after finishing the reaction. Thus, supporting heteropolyacid onto SiO_2 was performed in order to obtain a heterogeneous catalyst. Various amount (15-80 wt %) of 12-tungstophosphoricacid (HPW) was used in the impregnation of HPW on SiO_2 .

4.3.1.1.1 Structure and the composition of the materials

The XRD pattern of HPW/SiO_2 compared to that of HPW is presented in Figure 4.12.

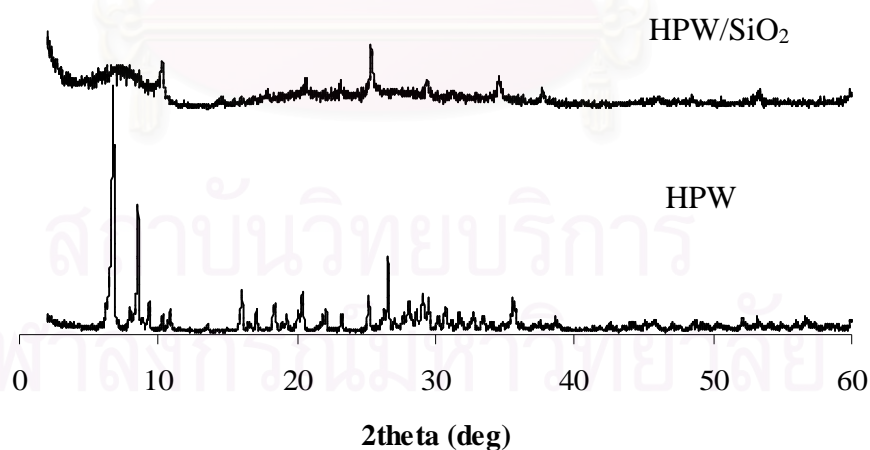


Figure 4.18 XRD Patterns of HPW and HPW/SiO_2 .

There were reflection patterns at $2q = 10.3, 25.4, 30.1, 36.8$ corresponding to HPW were observed [49]. Thus, the XRD pattern of HPW/SiO_2 showed existence of HPW on silica support.

4.3.1.1.2) Surface area and porosity of catalyst

Nitrogen sorption measurement is another method used for the determination of mesoporosity, surface area and pore size of materials, the specific surface area of both non-loaded and HPW loaded mesoporous silica was calculated using BET method. Their total pore volume was obtained from the desorption volume at $P/P_0 = 0.97$ and mean pore diameter was calculated from $4V_p/S$. The obtained N_2 sorption isotherms are display in Figure 4.19

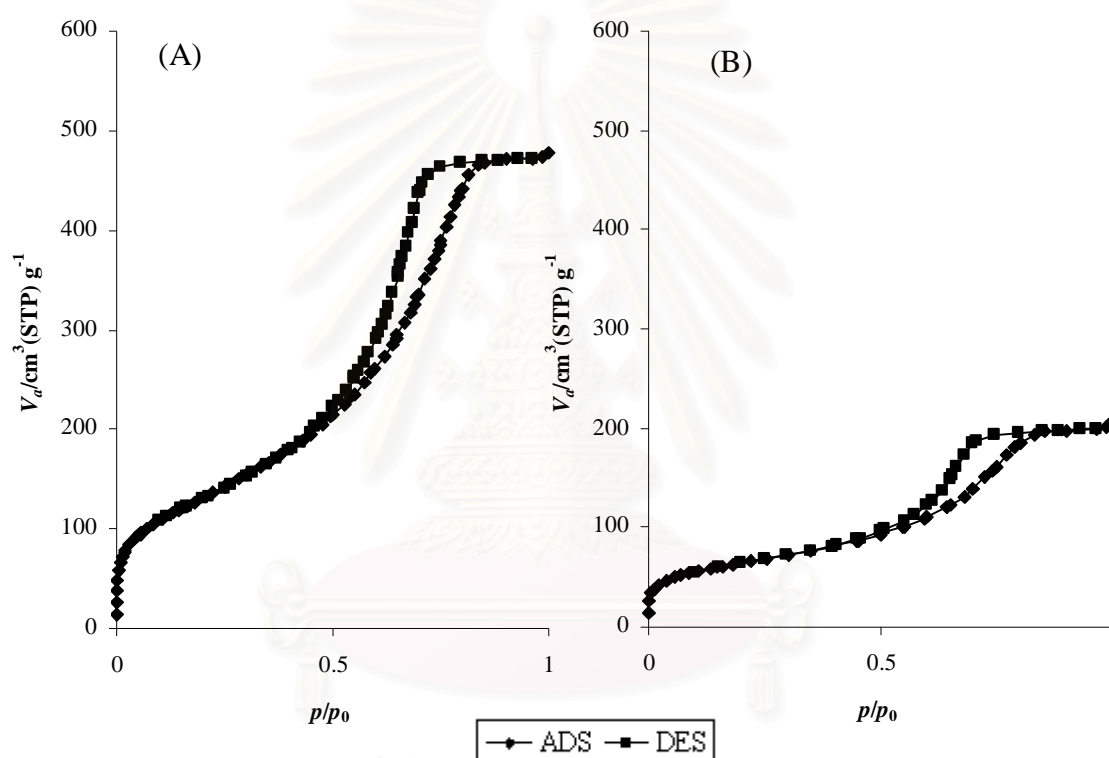


Figure 4.19 N_2 adsorption-desorption isotherm of (A) non-loaded mesoporous silica and (B) HPW loaded mesoporous silica

As seen from Figure 4.19, both material showed irreversible type IV adsorption isotherm with a H4 hysteresis loop as defined in the IUPAC [41]. A linear increase of adsorbed volume at low pressure followed by a steep increase in nitrogen uptake at a relative low pressure was observed. These phenomena were typically a characteristic of the capillary condensation inside the mesopore. This result was in

accordance with the previous work [50]. The textural properties obtained from N₂ sorption measurement are also summarized in Table 4.19.

Table 4.19 The textural properties of SiO₂ and HPW/SiO₂

Material	BET surface, S area (m²/g)	Total pore volume, V_p (cm³/g)	Mean pore diameter, MPD (nm)
SiO ₂	486	0.73	6
HPW/SiO ₂	228	0.31	5

S, BET surface are obtained from N₂ sorption; V_p, total pore volume obtained from single-point volume at $P/P_0 = 0.97$; MPD, mean pore diameter calculated from $4V_p/S$

The results revealed that impregnation of HPW resulted in a decrease in BET surface area resulting from HPA was located within mesoporous silica. This is in good agreement with the results reported previously [50].

4.3.1.1.3) Acidity properties of catalysts

Ammonia adsorption-desorption technique usually enables the determination of the strength of acid sites present on the catalyst surface together with total acidity. The NH₃-TPD profiles of different catalysts are shown in Figure 4.20.

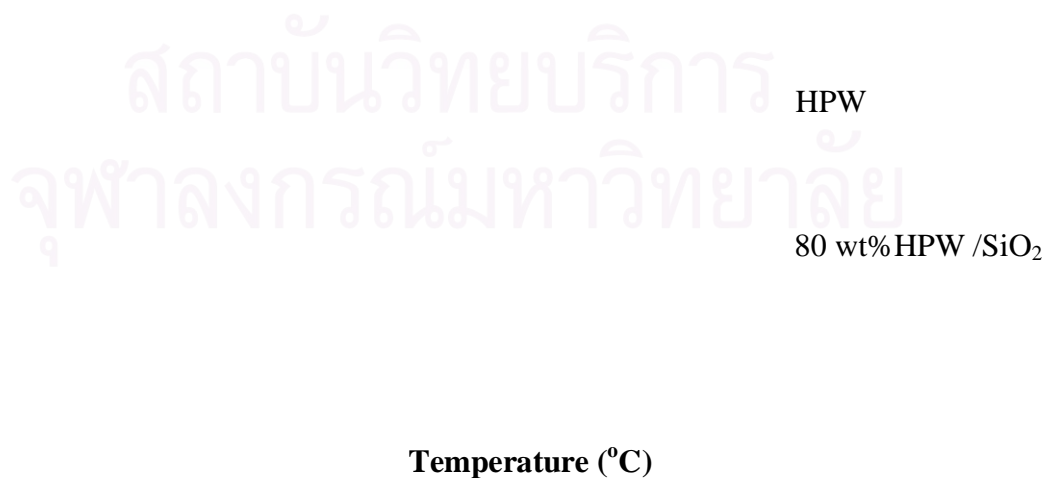


Figure 4.20 NH₃-TPD of HPW and 80 wt% HPW/SiO₂.

NH_3 desorbed from HPW at temperatures around 165°C and 575°C . The desorption pattern of 80 wt% HPW/ SiO_2 resembled that of pure HPW but with lower acidity. The total acidity is presented in Table 4.20.

Table 4.20 The total acidity of HPW and HPW/ SiO_2

Catalysts	Total acidity ($\text{mmol NH}_3 \text{ g}^{-1} \text{ cat}$)	Weak acidity: Brønsted acidity ($\text{mmol NH}_3 \text{ g}^{-1} \text{ cat}$)	Strong acidity: Lewis acidity ($\text{mmol NH}_3 \text{ g}^{-1} \text{ cat}$)
HPW	2.5593	1.4101	1.1492
HPW/ SiO_2	1.6558	0.8629	0.7923

4.3.1.1.4) Functional group of catalysts

The FT-IR spectrum of HPW/ SiO_2 is compared to that of HPW. The FT-IR spectra are shown in Figure 4.21.

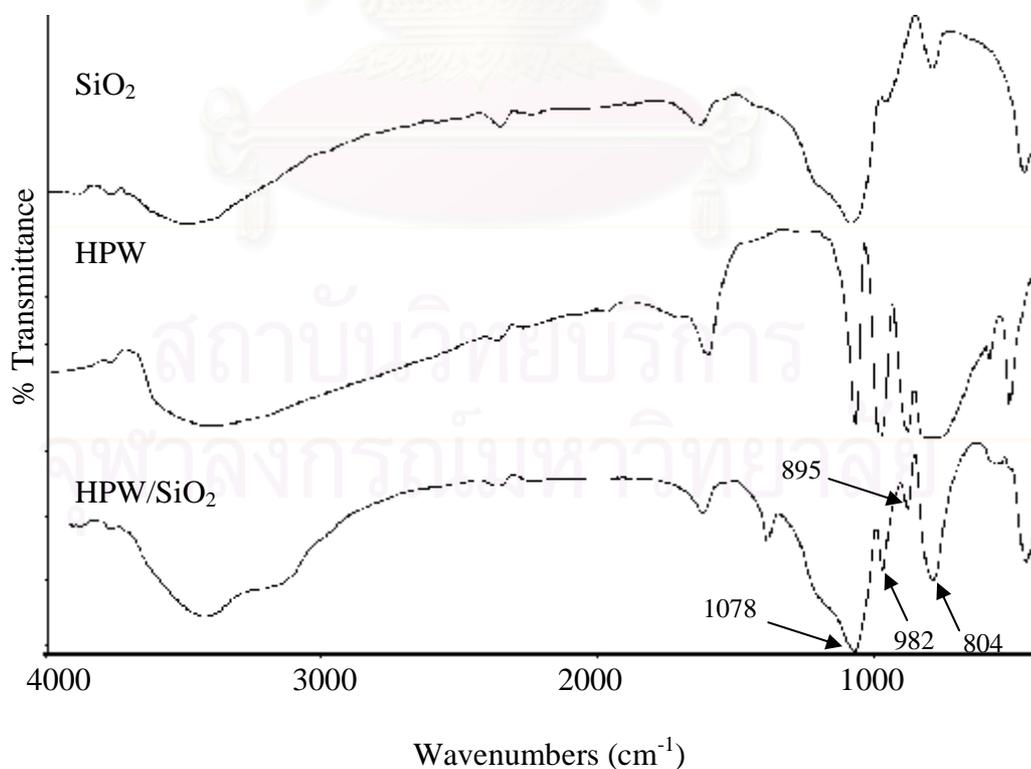


Figure 4.21 FT-IR spectra of SiO_2 , HPW and HPW/ SiO_2 .

The FT-IR spectrum of HPW/SiO₂ showed weak shoulder at 982 and 895 cm⁻¹ which were due to the W=O symmetric stretching band of HPW. Unfortunately, the bands at 1078 and 804 cm⁻¹ corresponding to the symmetric stretching of (P-O) and (W-O-W), respectively, were masked by stronger absorption of Si-O stretching and bending of silica, respectively, at the same wave numbers [51]. Therefore, FT-IR spectrum of HPW/SiO₂ indicated existence of HPW on silica support.

4.4 Crude rice bran oil

4.4.1 Fatty acid composition of crude rice bran oil

The crude rice bran oil was dark reddish brown in color. The fatty acid composition of crude rice bran oil was determined by method as describe in [38]. The results are shown in Table 4.21.

Table 4.21 Composition of crude rice bran oil

Fatty acid	(%)
C16:0 Palmitic acid	18.3
C18:0 Stearic acid	2.4
C18:1 Oleic acid	41.4
C18:2 Linoleic acid	37.9

It was found that the crude rice bran oil mainly consisted of unsaturated fatty acid, mainly oleic acid and linoleic acid. Free fatty acid content was determined by method as describe in [35] resulting 11.14%, which is far above the 1.0% limit for satisfactory transesterification reaction using alkaline catalyst leading to soap formation. The soap could prevent separation of the methyl ester layer from the glycerol fraction. An alternative method is to use acid catalysis, which are able to esterify free fatty acid. The esterification reaction stop in many cases due to the effect of the water produced when the free fatty acid react with methanol to form ester [31]. Therefore, the two step process, acid-catalyzed esterification process and followed by

base-catalyzed transesterification process were selected for converting crude rice bran oil to methyl ester of fatty acids.

4.4.2 Acid-catalyzed esterification of crude rice bran oil

The catalytic esterification of free fatty acid with methanol using different amount of HPW, and HPW/SiO₂ was carried out under the same reaction condition as methanol to oil molar ratio 10:1 using catalyst amount 2 wt% at 60°C for 3h. This reaction condition was similar to that used by *Siti et al.* [11]. The remaining free fatty acid after esterification reaction is indicated in Table 4.22.

Table 4.22 The remaining free fatty acid after esterification reaction.

Entry	Catalyst	Remaining FFA	FFA conversion
		(%)	(%)
1	HPW	1.08	90.3
2	15 wt% HPW/SiO ₂	6.28	43.6
3	30 wt% HPW/SiO ₂	5.00	55.1
4	80 wt% HPW/SiO ₂	1.78	84.2

Reaction Condition: methanol/oil molar ratio 10:1, catalyst amount 2 wt%, reaction time 3 h, reaction temperature 60°C.

The comparative catalytic activity of unsupported and supported HPW indicated that HPW gave higher FFA conversion than all of HPW/SiO₂. However, HPW was soluble in methanol and unable to be separated from reaction. In this work, heterogeneous catalyst was preferred. The data from Table 4.22 presented that increasing of HPW from 15-80 wt% onto SiO₂, the catalytic activity was increased obviously and came up to its maximum of 84.2% conversion using of 80 wt% HPW/SiO₂ catalyst. Therefore, the 80 wt% HPW/SiO₂ catalyst was chosen to use for esterification of free fatty acid in crude rice bran oil.

4.4.3 Influence of reaction parameters on esterification of free fatty acid

The parameters affecting the esterification reaction studied in this work were the amount of the catalyst, reaction temperature and reaction time. Methanol to oil ratio = 10 was chosen following the ratio used in the literature [2] indicating high free fatty acid conversion.

A. Effect of reaction temperature

Reaction temperature could influence the reaction rate. In this work, the reaction temperature was varied within a range from 60-90°C. The effect of reaction temperature on FFA concentration is shown in Figure 4.22.

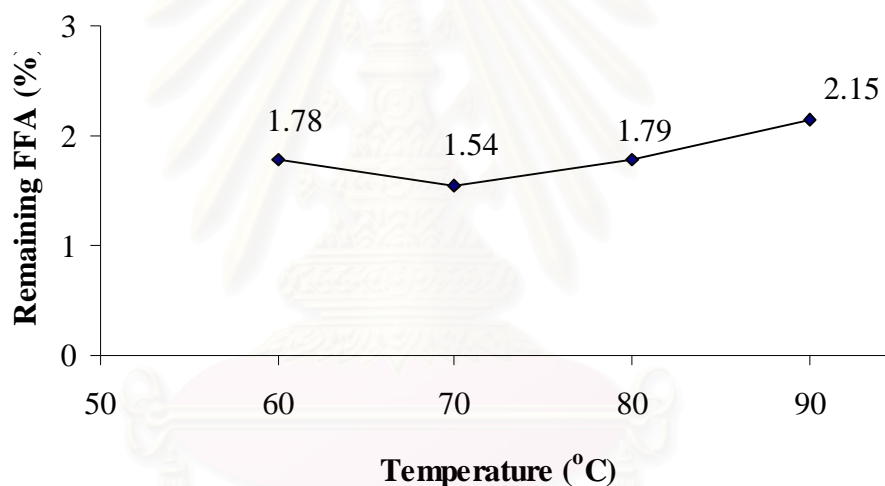


Figure 4.22 Remaining FFA as a function of reaction temperature.

Reaction condition: methanol to oil molar ratio = 10, reaction time 3 h and catalyst amount 2 wt%.

When esterification reaction was carried out at temperature 60 to 70°C, the remaining free fatty acid was decreased. However, with further increase temperature to reaction, the remaining free fatty acid was increased. At higher temperature than boiling point of methanol (65°C) triglyceride is hydrolyzed to free fatty acid. Therefore, the optimum reaction temperature for esterification of free fatty acid in crude rice bran oil was 70°C.

B. Effect of amount of catalyst

The effect of the catalyst amount was studied at a 10:1 molar ratio of methanol to oil at 70°C for 3 h. The catalyst amount was varied in the range of between 2.0 wt% and 5.0 wt%. The effect of amount of catalyst on FFA concentration is shown in Figure 4.23.

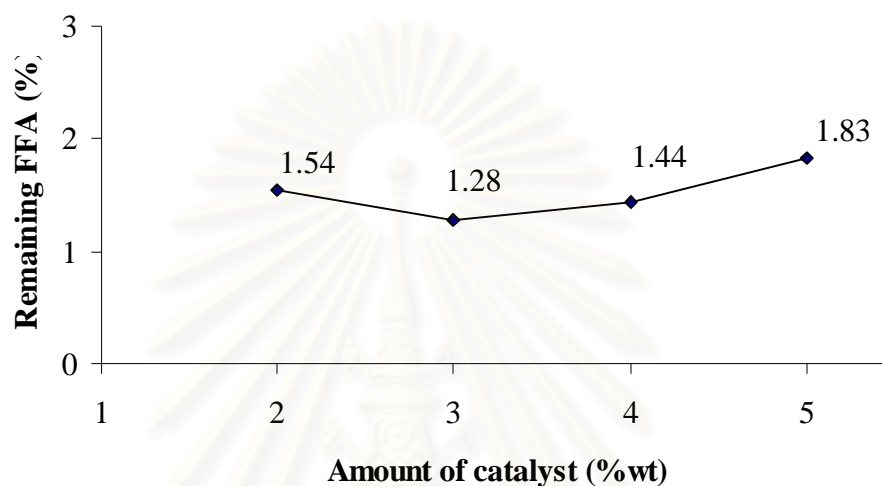


Figure 4.23 Remaining FFA as a function of amount of catalyst.

Reaction Condition: methanol to oil molar ratio = 10, reaction time 3 h and reaction temperature 70°C.

The results indicated that FFA concentration was influenced by the quantity of catalyst. By increasing the catalyst amount from 2 to 3wt%, the remaining free fatty acid was decreased to 1.28%. However, with further increase in the catalyst amount, the remaining free fatty acid was increased. Accordingly, the reaction was further studied with 3%wt of the catalyst for optimization of reaction time.

C. Effect of reaction time

The effect of reaction time was determined by performing reaction at varying reaction time in the range 3-6 h. The results are shown in Figure 4.24.

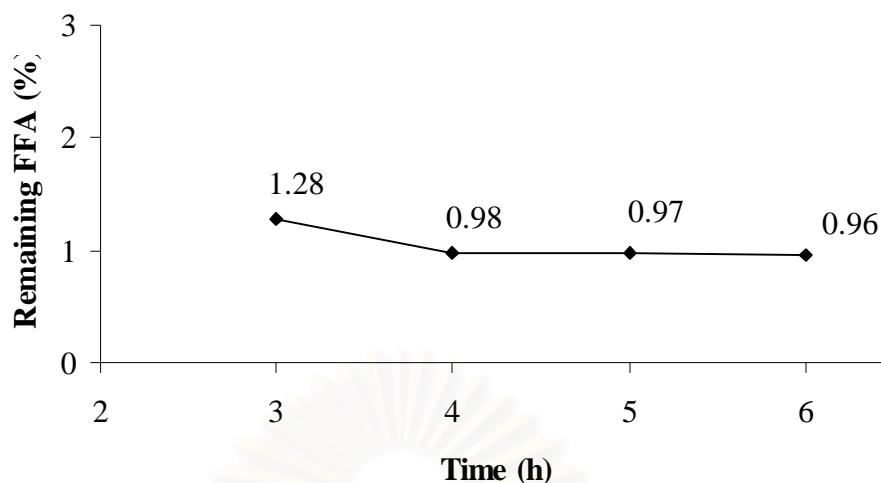


Figure 4.24 Remaining FFA as a function of reaction time.

Reaction Condition: methanol to oil molar ratio = 10, catalyst amount 3 wt% and reaction temperature 70°C.

As can be seen, the remaining free fatty acid was decreased with the reaction time, and in 4 h the remaining free fatty acid is 0.98%.

The objective of this stage was to reduce the free fatty acid in crude rice bran oil. It can be concluded that for the esterification of free fatty acid in rice bran oil with methanol, 80 wt% HPW/SiO₂ was found effective as catalyst. The reaction was carried out at 70°C for 4h with a molar ratio of crude rice bran oil to methanol of 10:1 using 3 wt% of catalyst which could reduce the free fatty acid level of crude rice bran oil to less than 1.0%.

4.5 Base catalyzed transesterification of treated rice bran oil

Successful base catalyzed transesterification process requires lower free fatty acid content in crude rice bran oil, which is less than 1%. After acid catalyzed esterification, the free fatty acid content in crude rice bran oil was less than 1%. Thus, in this step, base catalyzed transesterification was performed. The rehydrated Mg(Al)La hydrotalcite (La low) was chosen as a catalyst (from section 4.2.2.3) of transesterification reaction of the treated rice bran oil. The parameters affecting the

transesterification reaction studied in this work were the methanol to oil molar ratio and the catalyst amount.

A. Effect of methanol to oil molar ratio

The effect of methanol to oil molar ratio on ester content and product yield when reaction time was 9 h was performed. Excess methanol was needed even though theoretically the stoichiometry of the reaction requires 3 mol of methanol per mol of oil. This is generally ascribed to the chemical equilibrium shift. The improved oil solubility in an excess of alcohol could also favor the reaction [44]. The effect of methanol to oil molar ratio is presented in Table 4.23.

Table 4.23 Transesterification of treated rice bran oil as a function of methanol/oil molar ratio

Entry	CH ₃ OH/Oil molar ratio	Ester content (%)	Product yield (%)
1	15	65	75
2	30	100	74
3	45	100	49

Reaction Condition: Catalyst 7.5 wt% (based on rice bran oil), reaction temperature 100°C and reaction time 9 h

When the methanol to oil molar ratio was increased from 15 to 30, the ester content and product yield was increased considerably. The maximum methyl ester content was obtained at methanol to oil molar ratio = 30. At methanol to oil molar ratio = 45, the methyl ester content was not increased. Thus, methanol to oil molar ratio = 30 was sufficient for the treated rice bran oil transesterification under the reaction condition.

B. Effect of catalyst amount

In the case of homogeneous catalysts, it has been reported that the amount of catalyst has a strong influence on the conversion to methyl ester [27]. Therefore, the effect of catalyst amount was studied at a 30:1 molar ratio of methanol to oil at 100°C for 9 h. The results are shown in Table 4.24.

Table 4.24 Transesterification of treated rice bran oil as a function of catalyst amount

Entry	wt% catalyst	Ester content (%)	Product yield (%)
1	2.5	51	39
2	5.0	62	47
3	7.5	100	75
4	10.0	82	61

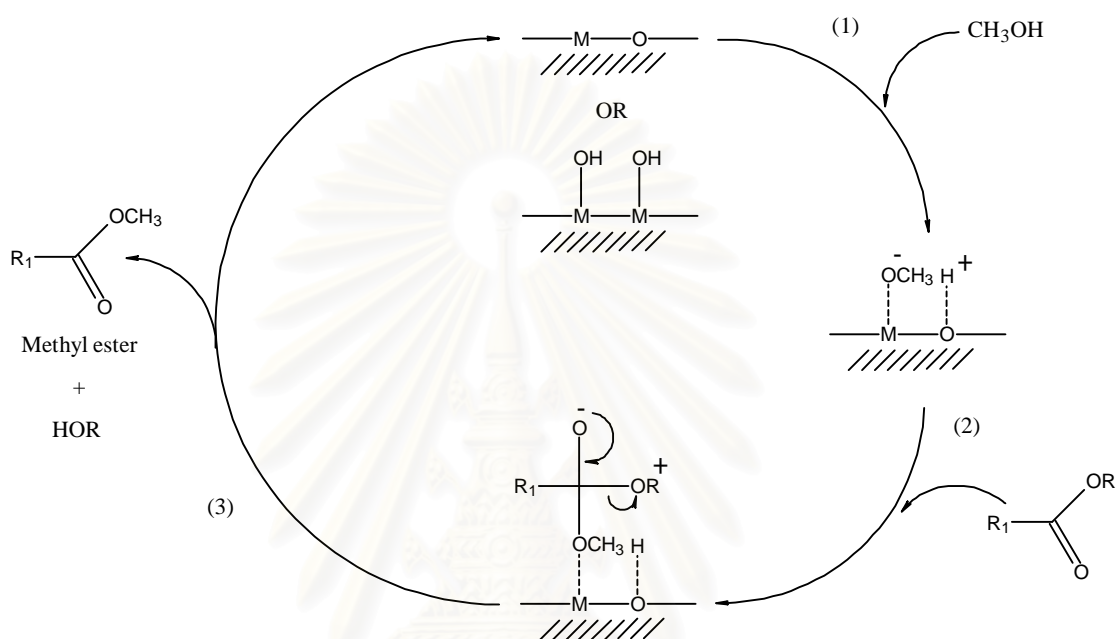
Reaction Condition: methanol to oil molar ratio 30:1, reaction temperature 100°C and reaction time 9 h.

The result indicated that the transesterification reaction was dependent upon the catalyst amount. The methyl ester content was increased with the increase of catalyst amount from 2.5 to 7.5 wt%, methyl ester content was from 51% to 100%. However, with further increase in the catalyst amount from 7.5wt% (oil 4.27 g, catalyst amount 0.32 g) to 10.0wt% (oil 4.27 g, catalyst amount 0.43) the methyl ester content was decreased, which was possibly due to mixing problem of reactant, product and solid catalyst.

It can be concluded that 100% methyl ester content was achieved using a 30:1 molar ratio of treated rice bran oil to methanol and catalyst amount 7.5 wt% at temperature 100°C for 9 h.

4.6 Proposed mechanism

The mechanism of base catalyzed methanolysis of ester for glyceryl tributyrate and rice bran oil using metal loaded mixed oxide and rehydrated Mg(Al)La hydrotalcite is proposed in Scheme 1.



Scheme 1. Mechanism of base-catalyzed transesterification of oil.
(where R_1 represents the long chain alkyl group)

In step (1), surface O^{2-} and/or OH^- extracts H^+ from CH_3OH to form surface CH_3O^- , which is strongly basic and has high catalytic activity in the transesterification reaction.

In step (2), the carbonyl carbon atom of the triglyceride molecule attracts a methoxide anion from the surface of the catalyst to form an intermediate. The intermediate reacts with methanol to generate methoxide anions.

In step (3), rearrangement of the intermediate results in the formation of biodiesel.

4.7 Comparison with other works.

A variety of solid base including basic zeolites, metal carbonates, supported alkali metal ions and alkali earth oxide, have been tested for biodiesel synthesis. By contrast, the base form of the titanolilicate ETS-10 [4] with microporous structure and supported alkali metal ions presented promising activity for the methanolysis of triglyceride even at low temperature. The high catalytic performance of ETS-10 and supported alkali metal ions, however, the resulted of alkali methoxide leaching, indicating to homogeneous catalysis was also detected [52]. Furthermore, catalysis in heterogeneous system still requires much of catalyst amount, methanol to oil molar ratio and reaction time. The comparisons of the result from this work with other works are presented in Table 4.25.

Table 4.25 Comparison of the result from this work with other works

Oil	Catalyst	Condition	Ester content (%)	Conversion (%)	Ref
Crude rice bran oil	Rehydrated Mg(Al)La hydrotalcite (low La)	T = 100°C t = 9 h Cat = 7.5wt% CH ₃ OH/oil molar ratio = 30	100	-	This work
Refined soybean	MgAlO	T = 60°C t = 9 h Cat = 7.5wt% CH ₃ OH/oil molar ratio = 15	-	67	[24]
Refined palm	1.5% K MgAlO	T = 100°C t = 9 h Cat = 7.5wt% CH ₃ OH/oil molar ratio = 45	94	-	[38]
Refined soybean	35% K/Al ₂ O ₃	T = 65°C t = 7 h Cat = 6.5wt% CH ₃ OH/oil molar ratio = 15	87	-	[44]

CHAPTER V

CONCLUSION AND SUGGESTIONS

The metal loaded mixed oxide catalyst with vary metal (K, Cs, Sr, Ba, La) prepared via impregnation method and hydrotalcite modified by La prepared via co-precipitation method was subjected to use as base catalyst in transesterification reaction. Transesterification of glyceryl tributyrate (as a model compound of oil) with methanol was studied in order to compare catalytic activity of the prepared heterogeneous base catalysts. The results show that among the metal loaded MgAlO catalysts, 1.5%K MgAlO (Mg/Al molar ratio = 4) catalyst gives the highest conversion of glyceryl tributyrate but metal leaching was also detected from the catalyst. Comparison between Mg(Al)LaO and rehydrated Mg(Al)La hydrotalcites the results show that the rehydrated catalyst is more active than Mg(Al)LaO. Moreover, the amount of La in the catalysts effect to metal leaching from catalyst indicating that the high amount of La gives higher metal leaching. Therefore, the rehydrated Mg(Al)La hydrotalcite (La low) was proper as a base catalyst for the transesterification of crude rice bran oil containing high free fatty acid (11.14% FFA).

For the acid catalyzed esterification reaction, HPW loaded on mesoporous silica was prepared by impregnation method. The results show that the 80wt% HPW/SiO₂ gives the highest free fatty acid conversion. A study into the effect of the reaction condition of esterification of free fatty acid in crude rice bran oil was performed, it can be concluded that at 70°C for 4 h with methanol to oil molar ratio = 10 using 3wt% of catalyst leads to remaining free fatty acid less than 1.0%. Then, the base catalyzed transesterification of treated rice bran oil with methanol was performed using the rehydrated MgAlLa hydrotalcire (La low) catalyst. A 30:1 molar ratio of methanol to oil, amount of catalyst 7.5 wt%, reaction temperature 100°C and reaction time 9 h, which resulted in 100% ester content and 74% product yield.

Suggestion for the future work

From all aforementioned results, the future work should be focused on the following:

1. Hydrotalcite with higher molar ratio of Mg/Al should be tested and compared.
2. The modification of hydrotalcites through addition of other cation (Sm, Gd, Dy) should be investigated.



สถาบันวิทยบริการ
จุฬาลงกรณ์มหาวิทยาลัย

REFERENCES

1. Thai Parliament 2002. Alternative fuels: ethanol and biodiesel.
2. Wang, Y.; Ou, S.; Liu, P.; and Zhang Z. Preparation of biodiesel from waste cooking oil via two-step catalyzed process. Energ. Convers. Manage. 48 (2007): 184-188.
3. Peterson, G.; Scarah, W. Rapeseed oil transesterification by heterogenous catalyst. J. Am. Oil Chem. Soc. 61 (1984): 1593-1597.
4. Suppes, G. J.; Dasari, M. a.; and Doskocil, E. J. Transesterification of soybean oil with zeolite and metal catalyst. J. Catal. A. 257 (2004): 213-223.
5. Cavani, F.; Trifiro, F.; and Vaccari, A. Hydrotalcite-type anionic clays: Preparation, properties and application. Catal. Today 11 (1991): 173-301.
6. Lin, C.Y.; Lin, H.A.; and Hung, L.B. Fuel structure and properties of biodiesel produced by the peroxidation process. Fuel 85 (2006): 1743-1749.
7. Arabi, M.; Amini, M.M.; Abedini, M.; Nemati, A.; and Alizaden, M. Esterification of phthalic anhydride with 1-butanol and 2-ethylhexanol catalyzed by heteropolyacids. J. Mol. Catal. A: Chem. 200 (2003): 105-110.
8. Patel, S.; Purohit, N. and Patel, A. Synthesis, characterization and catalytic activity of new solid acid catalysts, $H_3PW_{12}O_{40}$ supported on to hydrous zirconia. J. Mol. Catal. A: Chem. 192 (2003): 195-202.
9. Roy, A.; Forana, C.; Malki, K.E.; and Bess, J.P. Expanded clays and other microporous solids. Vol. 2. New York: Reinhold (1992): 108-169.
10. Cantrell, D. G.; Gillie, L. J.; and Lee, A. F. Structure-reactivity correlations in MgAl hydrotalcite catalysts for biodiesel synthesis. Appl. Catal. A. 287 (2005): 183-190.
11. Siti, Z.; Lai, C.C.; Vali. S.R.; and Ju, Y.H. A two-step acid-catalyzed process for the production of biodiesel from rice bran oil. Biores. Technol. 96 (2005): 1889-1896.
12. Freedman, B.; Butterfield, R. O.; and Pryde, E. H. Transesterification kinetics of soybean oil. JAOC 63 (1986): 1375-1380.
13. Lapprasert, N. Synthesis of methyl ester from used cooking oils. Master's Thesis, Program of Petrochemistry and Polymer Science, Faculty of Science, Chulalongkorn University, 2005.

14. Wright, H. J.; Segur, J.B.; Clark, H.V.; Coburn, S.K.; Lang-don, E.E.; and DuPuis, R.N. A report on ester interchange. Oil and Soy (1944): 145-148.
15. Kuadina, D.; and Saka, S. Biodiesel fuel from rapeseed oil as prepared in supercritical methanol. Master's Thesis, Department of Chemistry, Faculty of Science, Kyoto University, 2001.
16. Tomasevic, A. V.; and Siler-Marinkovic, S. S. Methanolysis of used frying oil. Fuel Process. Technol. 81 (2003): 1–6.
17. Felizardo, P; Correia, M.J.N.; Raposo, I.; Mendes, J.F.; Berkemeier, R.; and Bordado, J.M. Production of biodiesel from waste frying oils. Waste Manage. 26 (2006): 487-494.
18. Choudary, B. M.; Kantam, M.L.; Reddy, C.V.; Aranganathan, S.; Santhi, P.L.; and Figueras, F. Mg–Al–O–t-Bu hydrotalcite: a new and efficient heterogeneous catalyst for transesterification. J. Mol. Catal. A: Chem. 159 (2000): 411–416.
19. Kim, H. J.; Kang, B. S.; Kim, M. J.; and Lee, J. S. Transesterification of vegetable oil to biodiesel using heterogeneous base catalyst. Catal. Today 93 (2004): 315-320.
20. Furuta, S.; Matsushashi, H.; and Arata, K. Biodiesel fuel production with solid amorphous-zirconia catalysis in fixed bed reactor. Biomass Bioenerg. 30 (2006): 870–873
21. Bitjega. R.; Pavel. O.D.; Costentin, G.; Che. M.; and Angelescu, E. Rare-earth elements modified hydrotalcites and corresponding mesoporous mixed oxides as basic solid catalysts. Appl. Catal. A. 288 (2005): 185-193.
22. Sepúlveda, J.H.; Yori, J.C.; and Vera, C.R. Repeated use of supported $H_3PW_{12}O_{40}$ catalysts in the liquid phase esterification of acetic acid with butanol. Appl. Catal. A. 288 (2005): 18-24.
23. Huaping, Z.; Zongbin, W.; Yuanxiong, C.; Ping, Z.; Shijie, D.; Xiaohua, L.; and Zongqiang, M. Preparation of Biodiesel Catalyzed by Solid Super Base of Calcium Oxide and Its Refining Process. Chin. J. Catal. A. 27 (2006): 391-396.
24. Xia, W.; Peng, H.; and Chen, L. Calcined Mg-Al hydrotalcites as solid base catalysts for methanolysis of soybean oil. J. Mol. Catal. A: Chem. 246 (2006): 24-32.

25. Liu, X.; He, H.; Wang, Y.; and Zhu, S. Transesterification of soybean oil to biodiesel using SrO as a solid base catalyst. Catal. Commun. 8 (2007): 1107-1111.
26. Xie, W.; Huang, X.; and Li, H. Soybean oil methyl esters preparation using NaX zeolites loaded with KOH as a heterogeneous catalyst. Biores. Technol. 98 (2007): 936-939.
27. Yang, Z.; and Xie, W. Soybean oil transesterification over zinc oxide modified with alkali earth metals. Fuel Process. Technol. 88 (2007): 631-638.
28. MacLeoda, C.S.; Harvey, A.P.; Lee, A.F.; and Wilson, K. Evaluation of the activity and stability of alkali-doped metal oxide catalysts for application to an intensified method of biodiesel production. J. Chem. Eng. 135 (2008): 63-70.
29. Ghadge, S.V.; and Raheman, H. Biodiesel production from mahua (*Madhuca indica*) oil having high free fatty acids. Biomass Bioenerg. 28 (2005): 601-605.
30. Ramadhas, A.S.; Jayaraj, S.; and Muraleedharan, C. Biodiesel production from high FFA rubber seed oil. Fuel 84 (2005): 335-340.
31. Berchmans, H.J.; and Hirata, S. Biodiesel production from crude *Jatropha curcas* L. seed oil with a high content of free fatty acids. Biores. Technol. 99 (2008): 1716-1721.
32. Di Cosimo, J.I.; Diez, V.K.; and Apesteguia, C.R. Base catalysis for the synthesis of α,β -unsaturated ketones from the vapor-phase aldol condensation of acetone. Appl. Catal. A. 137 (1996): 149-154.
33. Wang, Y.; Han, X. W.; Ji, A.; Shi, L.Y.; and Hayashi, S. Basicity of potassium-salt modified hydrotalcite studied by ^1H MAS NMR using pyrrole as a probe molecule. Micropor. Mesopor. Mater. 77 (2005): 139-145.
34. Soled, S.; Miseo, S.; McVicker, G.; Gates, W.E.; Gutierrez, A.; and Paes, J. Preparation of bulk and supported heteropolyacid salts. Catal. Today 36 (1997): 441-450.
35. Saad, B.; Ling, C. W., Jab M. S.; Lim, B. P.; Ali, A. S. M.; Wai, W. T.; and Saleh, M. I. Determination of free fatty acid in palm oil sample using non-aqueous flow injection titrimetric method. Food Chem. 4 (2007): 1407-1414.

36. Wu, G.; Wang, X.; Chen, B.; Li, J.; Zhao, N.; Wei, W.; and Sun, Y. Fluorine-modified mesoporous Mg-Al mixed oxide: Mild and stable base catalysts for *O*-methylation of phenol with dimethyl carbonate. J. App. Catal. A: Gen. 329 (2007): 106-111.
37. Tao, Q.; Zhang, Y.; Zhang, X.; Yuan, P.; and He, H. Synthesis and characterization of layered double hydroxides with a high aspect ratio. J. Solid State Chem. 179 (2006): 708-715.
38. Tittabutr, T. Hydrotalcite base catalysts for biodiesel production. Master's Thesis, Program of Petrochemistry and Polymer Science, Faculty of Science, Chulalongkorn University, 2006
39. Xie, W.; and Yang, Z. Ba-ZnO catalysts for soybean oil transesterification. Catal. Lett. 117 (2007): 159-165.
40. Reichle, W.T.; Kang, S.Y.; and Everhardt, D.S. Natural of the thermal decomposition of a catalytically active anionic clay mineral. J. Catal. 101 (1986): 352-359.
41. Sing, K.S.W.; Everet, D.H.; Haul R.A.W.; Moscou, L.; Pierotti, R.A.; Rouquerol, J.; and Siemieniewska, T. Reporting physisorption data for gas/solid system with special reference to the determination of surface area and porosity. Pure. App. Chem. 57 (1985): 603-619.
42. Kustrowski, P.; Chmielarz, L.; Bozek, E.; Sawalha, M.; and Roessner, F. Acidity and basicity of hydrotalcite derived mixed Mg-Al oxides studied by test reaction of MBOH conversion and temperature programmed desorption of NH₃ and CO₂. Mater. Res. Bull. 39 (2004): 263-281.
43. Narayanan, S.; and Krishna, K. Structure activity relationship in Pd/hydrotalcite: effect of calcination of hydrotalcite on palladium dispersion and phenol hydrogenation. Catal. Today 49 (1999): 57-63.
44. Xie, W.; Peng, H.; and Chen, L. Transesterification of soybean oil catalyzed by potassium loaded on alumina as a solid-base catalyst. Appl. Catal. A: Gen. 300 (2006): 67-74.
45. Angelescu, E.; Pavel, O.D.; Che, M.; Birjega, R.; and Constantin, G. Cyanoethylation of ethanol on Mg-Al hydrotalcites promoted by Y³⁺ and La³⁺. Catal. Commun. 5 (2004): 647-651.
46. Occelli, M.L.; Olivier, J.P.; Auroux, A.; Kalwei, M.; and Eckert, H. Basicity and porosity of a calcined hydrotalcite-type material from nitrogen porosimetry

- and adsorption microcalorimetry methods. Chem. Mater. 15 (2003); 4231-4238.
47. Xi, Y.; and Davis, R.J. Influence of water on the activity and stability of activated Mg-Al hydrotalcites for the transesterification of tributyrin with methanol. J. Catal. 254 (2008):190-197.
48. Alonso, D.M.; Mariscal, R.; Tost, R. M.; Poves, M.D.Z.; and Granados, M.L. Potassium leaching during triglyceride transesterification using K/ γ -Al₂O₃ catalysts. Catal. Commun 8 (2007): 2074-2080.
49. Juan, J.H; Zhang, J.; and Yarmo, M.A. 12-Tungatophosphoric acid supported on MCM-41 for esterification of fatty acid under solvent free condition. J. Mol. Catal. A: Chem. 267 (2007): 265-271.
50. Lapkin, A.; Bozkaya, B.; Mays, T.; Borello, L.; Edler, K.; and Crittenden, B. Preparation and characterization of chemisorbents based on heteropolyacid supported on synthetic mesoporous carbon and silica. Catal. Today 81 (2003): 611-621.
51. Sharma, P.; Vyas, S.; and Patel, A. Heteropolyacid supported onto neutral alumina: characterization and esterification of 1^o and 2^o alcohol. J. Mol. Catal. A: Chem. 217 (2004): 281-286.
52. Lopez, J.C.; Goodwin, J.G.; Bruce, D.A.; and Lotero, E. Transesterification of triacetin with methanol on solid acid and base catalysts. Appl. Catal. A: Gen. 295 (2005): 97-105.



APPENDICES

สถาบันวิทยบริการ
จุฬาลงกรณ์มหาวิทยาลัย

APPENDIX A

GC-MS of liquid mixture from glyceryl tributyrate transesterification

The mixture from reaction was analyzed by GC-MS. The results are shown in Fig. A-1

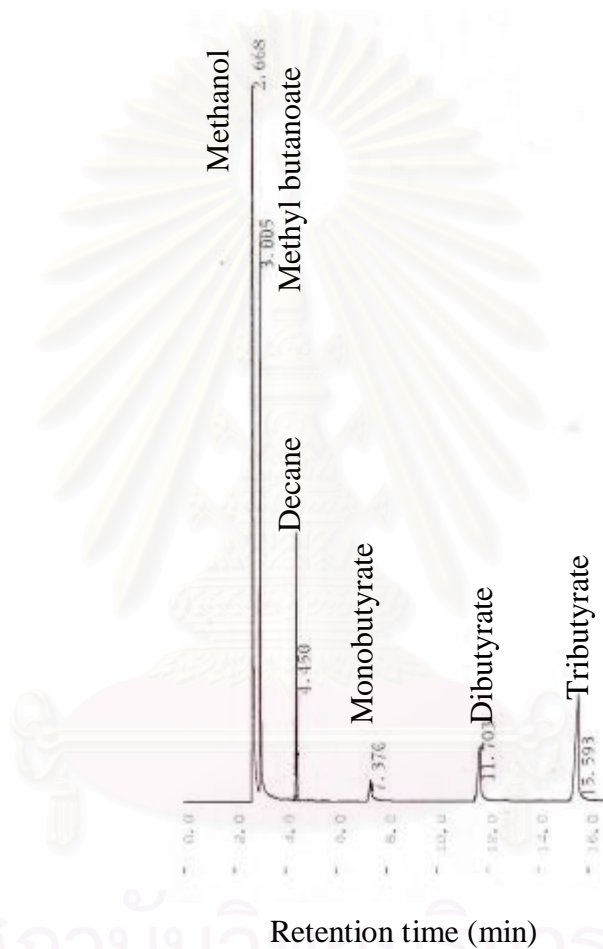


Figure A-1 Gas chromatogram of liquid product from reaction mixture of transesterification of glyceryl tributyrate.

GC calculation

The conversion of glyceryl tributyrate was analyzed by gas chromatography using standard method.

Calculation of the correction factor

The correction factor mixture was prepared by added glyceryl tributyrate 1.5 mL (5.1×10^{-3} mol) in 6.25 mL of methanol then filtration. The internal standard was added to 1 mL of filtrate before was analyzed by GC. The correction factor was calculated based upon the results obtained from gas chromatographic analysis. Decane was used as internal standard.



Figure A-2 Gas chromatogram of liquid mixture for correction factor calculation.

Exact amount of glyceryl tributyrate = 5.1×10^{-3} mol

Exact amount of internal standard = 0.102×10^{-3} mol

Peak area of glyceryl tributyrate = 84428

Peak area of internal standard = 13683

Total volume of the reaction = 7.75 ml

The calculation of the correction factor is described as follows:

The amount of glyceryl tributyrate from the reaction mixture

$$\frac{\text{Amount of decane (mol)}}{\text{Peak area of decane}} = \frac{\text{Amount of glyceryl tributyrate}}{\text{Peak area of glyceryl tributyrate}}$$

$$\frac{0.102 \times 10^{-3} \text{ mol}}{13683} = \frac{\text{Amount of glyceryl tributyrate}}{84428}$$

Amount of glyceryl tributyrate = 0.629×10^{-3} mol

The amount of glyceryl tributyrate in total volume of the mixture (mL)

$$= \text{Amount of glyceryl tributyrate} \times \text{total volume of the mixture}$$

$$= 0.629 \times 10^{-3} \text{ mol} \times 7.75 \text{ mL}$$

$$= 4.88 \times 10^{-3} \text{ mol}$$

Thus, the correction factor of glyceryl tributyrate is calculated as:

$$= \frac{\text{Exact amount of glyceryl tributyrate}}{\text{Amount of glyceryl tributyrate mixture}}$$

$$= \frac{5.1 \times 10^{-3} \text{ mol}}{4.88 \times 10^{-3} \text{ mol}}$$

$$= 1.05$$

Correction factor of glyceryl tributyrate was 1.05.

Calculation of %conversion of glyceryl tributyrate

At the end of the reaction, the catalyst was separated by filtration. Then, the internal standard was added to 1 mL of filtrate before was analyzed by GC. The conversion was calculated based upon the results obtained from gas chromatographic analysis. Decane was used as internal standard.

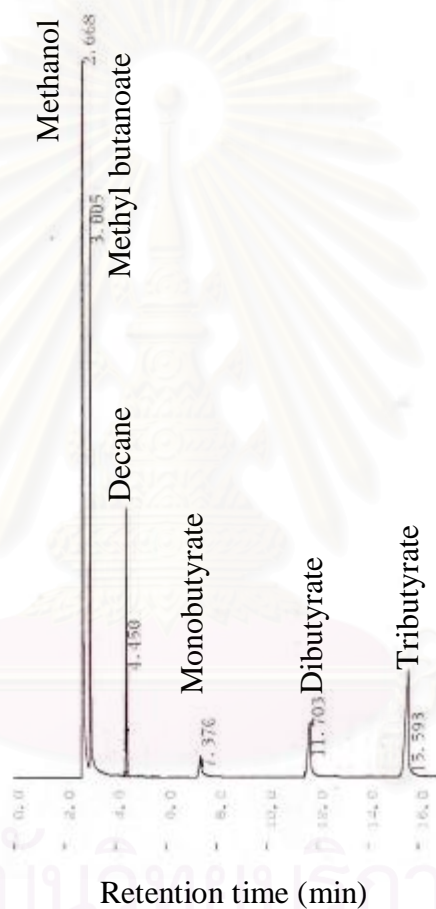


Figure A-3 Gas chromatogram of liquid product from reaction mixture of transesterification of glyceryl tributyrate using 1.5 wt% MgAlO catalyst.

- A: exact amount of glyceryl tributyrate = 5.1×10^{-3} mol
- B: exact amount of internal standard = 0.102×10^{-3} mol
- C: peak area of glyceryl tributyrate = 29968
- D: peak area of internal standard = 15447
- E: total volume of the reaction = 5.0 mL

The calculation of the correction factor is described as follows:

The amount of glyceryl tributyrate from the reaction mixture

$$\frac{\text{Amount of decane (mol)}}{\text{Peak area of decane}} = \frac{\text{Amount of glyceryl tributyrate}}{\text{Peak area of glyceryl tributyrate}}$$

$$\frac{0.102 \times 10^{-3} \text{ mol}}{15447} = \frac{\text{Amount of glyceryl tributyrate}}{29968}$$

$$\text{Amount of glyceryl tributyrate} = 0.19 \times 10^{-3} \text{ mol}$$

The amount of glyceryl tributyrate in total volume of the mixture (mL)

$$\begin{aligned} &= \text{Amount of glyceryl tributyrate} \times \text{total volume of the mixture} \\ &= 0.20 \times 10^{-3} \text{ mol} \times 5.0 \text{ mL} \\ &= 1.00 \times 10^{-3} \text{ mol} \end{aligned}$$

Multiply by correction factor

$$\begin{aligned} &= 1.00 \times 10^{-3} \text{ mol} \times 1.05 \\ &= 1.05 \times 10^{-3} \text{ mol} \end{aligned}$$

Thus, %conversion glyceryl tributyrate can be calculated as:

$$\begin{aligned} &= (5.1 \times 10^{-3} - 1.05 \times 10^{-3} \text{ mol}) / 5.1 \times 10^{-3} \text{ mol} \times 100 \\ &= 79\% \end{aligned}$$

Calculation of %ester content and product yield of crude rice bran transesterification

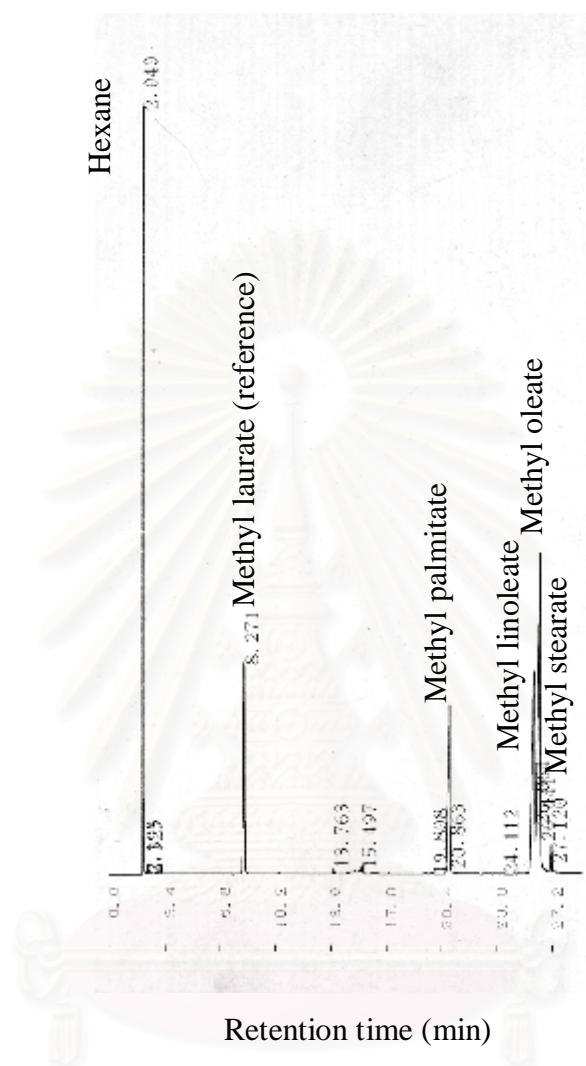


Figure A-4 Gas chromatogram of products from crude rice bran teansesterification.

The analysis of methyl ester was carried out by GC using methyl laurate as reference.

Methyl esters content (%)

Weight of reference was added = 0.0305 g

Weight of methyl ester was added = 0.2598 g

Peak area of reference (methyl laurate) = 9441

Peak area of methyl ester = 80191

$$\begin{aligned}
 &= \frac{(\text{weight of reference} \times \text{area of methyl esters}) \times 100}{\text{area of reference} \times \text{weight of methyl ester}} \\
 &= \frac{(0.0305 \times 80191) \times 100}{(9441 \times 0.2598)} \\
 &= 100 \%
 \end{aligned}$$

Product yield (%)

Weight of top phase = 3.22 g

$$\begin{aligned}
 &= \frac{(\text{weight of top phase} \times \% \text{ methyl esters content})}{\text{weight of crude rice bran oil used}} \\
 &= \frac{(3.22 \times 100)}{4.27} \\
 &= 75 \%
 \end{aligned}$$

สถาบันวิทยบริการ
จุฬาลงกรณ์มหาวิทยาลัย

VITAE

Ms. Patcharaporn Chuayplod was born on November 21th, 1983 in ChiangMai, Thailand. She received a Bachelor Degree of Science, major in Chemistry from Thammasat University in 2005. Since 2005 she has been a graduate student in the program of Petrochemistry and Polymer Science, Faculty of Science, Chulalongkorn University and graduated in 2007.

Her present address in 75/181, Songprapa Road, Srirung, Donmuang, Bangkok, Thailand 10210, Tel 0812794544



สถาบันวิทยบริการ
จุฬาลงกรณ์มหาวิทยาลัย